Paramoeba atlantica as a Natural Intracellular Niche for Vibrios in Marine Ecosystems

Laura Onillon, Anaïs Dufau, Vincent Delafont, Hajar Amraoui, Etienne Robino, Angélique Perret, Océane Romatif, Juliette Pouzadoux, Thierry Soldati, Marie-Agnès Travers, et al.

Environmental Microbiology

ENVIRONMENTAL MICROBIOLOGY

RESEARCH ARTICLE OPEN ACCESS

Paramoeba atlantica as a Natural Intracellular Niche for Vibrios in Marine Ecosystems

Laura Onillon[1] | Anaïs Dufau[1] | Vincent Delafont[2] | Hajar Amraoui[1] | Etienne Robino[1] | Angélique Perret[1,3] | Océane Romatif[1] | Juliette Pouzadoux[1] | Thierry Soldati[3] | Marie-Agnès Travers[1] | Guillaume M. Charrière[1]

[1]IHPE UMR 5244, University of Montpellier, CNRS, Ifremer, University of Perpignan Via Domitia, Montpellier, France | [2]EBI, UMR 7267, CNRS, University of Poitiers, Poitiers, France | [3]Département de Biochimie, Faculté des Sciences, Université de Genève, Sciences II, Genève, Switzerland

Correspondence: Guillaume M. Charrière (guillaume.charriere@umontpellier.fr)

Received: 27 March 2025 | **Revised:** 27 May 2025 | **Accepted:** 4 June 2025

Funding: The present study was supported, by the Ec2co-CNRS funded VibrAm and Vintage projects, by Labex CEMEB Reservib project, and by Ifremer, University of Montpellier and University of Perpignan via Domitia. This study is set within the framework of the 'Laboratoire d'Excellence (LabEx)' TULIP(ANR-10-LABX-41). Laura Onillon was supported by an Ifremer scholarship.

Keywords: intracellular niche | *Paramoeba* | vibrios | virulence

ABSTRACT

Vibrios are a group of aquatic bacteria that include diverse pathogens for humans and marine animals. In their natural environment, these bacteria are subject to predation by heterotrophic protozoa, including free-living amoebae. Previous studies suggested that some amoebae species can promote the environmental persistence and dissemination of pathogenic vibrios. However, most research has focused on model amoebae derived from freshwater habitats despite the prevalence and diversity of amoebae and vibrios in marine ecosystems. This study identifies a natural association between the marine amoeba *Paramoeba atlantica* and *Vibrio bathopelagicus,* a member of the Splendidus clade. Investigations at the cellular level revealed that *V. bathopelagicus* can resist digestion by *P. atlantica* and can swim and replicate in large digestive vacuoles for hours before being released by exocytosis. Furthermore, *V. bathopelagicus* exhibits virulence potential against oysters. Intravacuolar survival in *P. atlantica* was observed for various vibrios, and screening of clonally isolated free-living marine amoebae revealed that many Paramoebidae are found associated with vibrios. Our findings show that Paramoebidae can act as a widespread intracellular reservoir for diverse vibrios. This provides new insights into the environmental intracellular niches and opportunistic strategies of vibrios in marine ecosystems.

1 | Introduction

Vibrios constitute a group of highly diverse ɣ-proteobacteria ubiquitous in aquatic environments, ranging from freshwater to marine habitats. They are found in coastal to open waters (Thompson et al. 2004; Takemura et al. 2014) and can colonise a wide array of ecological niches due to their genetic plasticity and metabolic versatility (Le Roux et al. 2016). They can be associated with marine animals, planktonic organisms, (a)biotic particles, biofilms or persist in the water column in a free-living planktonic form (Lyons et al. 2007; Takemura et al. 2014; Thompson et al. 2004). Their associations with animals can lead to a spectrum of ecological relationships, from mutualistic symbiosis to pathogenic interactions. Some vibrios are known to cause diseases affecting humans (Harris et al. 2012) and marine animals including crustaceans, corals, fishes and molluscs (Destoumieux-Garzón et al. 2020; Goulden et al. 2012; Ina-Salwany et al. 2019; Kushmaro et al. 2001). In the oyster *Magallana gigas*, some vibrios are implicated in mass mortality episodes, leading to major economic losses in aquaculture

(Travers et al. 2015). Pathogenic vibrios in oysters include primary pathogens, such as *Vibrio aestuarianus* (Garnier et al. 2008; Mesnil et al. 2023) and opportunistic pathogens, the most studied belonging to the *Splendidus* and *Harveyi* superclades (Saulnier et al. 2010; Lemire et al. 2015; Rubio et al. 2019; Oyanedel et al. 2023). The virulence of these opportunistic vibrios primarily stems from diverse anti-eukaryote activities, such as cytotoxicity, disrupting oyster immune cells (i.e., haemocytes) function through species-specific molecular mechanisms (Rubio et al. 2019).

Acquisition of anti-eukaryote activities in bacteria can emerge in response to the selective pressure exerted by bacterial grazers. Among them, free-living amoebae (FLA) represent an important part of the heterotrophic protists preying on bacteria through phagocytosis in aquatic environments. In return, diverse bacteria have acquired mechanisms to escape or resist such predation and are referred to as amoeba-resisting bacteria, or endosymbionts if they have established a stable, long-term relationship with their amoebal host (Greub and Raoult 2004). Because the mechanisms of phagocytosis are highly conserved among distant organisms, these biotic interactions are believed to contribute to the selection of virulence traits against animal immune cells (Molmeret 2005; Boulais et al. 2010). FLA can also act as a reservoir and/or vector of pathogenic bacteria, supporting their environmental persistence, dissemination, and even providing a replicative niche (Fields et al. 1989; Berk et al. 1998; García et al. 2007; Cervero-Aragó et al. 2015).

Several studies have pointed out the potential role of amoeba-vibrio interactions in the environmental persistence of pathogenic vibrios and virulence acquisition. The human pathogen *V. cholerae* can establish a replicative niche within *Acanthamoeba castellanii* contractile vacuole (Van der Henst et al. 2016, 2018) and can replicate intracellularly in *Acanthamoeba polyphaga*, colonising uncharacterized vacuoles (Sandström et al. 2010). In addition, the opportunistic pathogen *V. parahaemolyticus* was shown to benefit from *A. castellanii* presence through uncharacterized compounds released by the amoeba (Laskowski-Arce and Orth 2008). Even though these findings provide important insights into the significance of these interactions in vibrio ecology, they mostly relied on the model FLA *A. castellanii* (Neff strain). More importantly, this FLA is not suited for studying marine bacteria because high salinities slow its multiplication rate, ultimately inducing encystment (Cordingley et al. 1996). Because most vibrio species are halophilic (Sampaio et al. 2022), extrapolating these observations to other vibrio species requires the use of FLA isolated from relevant ecological contexts. Additionally, most interactions studied so far are experimental and involve laboratory strains—of both amoebae and vibrios—rather than naturally associated partners, raising the question of the ecological accuracy of the described interactions.

We recently demonstrated that *Vibrio tasmaniensis* LGP32, an oyster pathogen, can resist predation by marine amoeba from the genus *Vannella* (Robino et al. 2020). Furthermore, we showed that these environmental FLA can naturally associate with vibrios (Robino et al. 2020), a finding that supports the ecological reality of amoeba–vibrio associations in the marine environment. The 18S barcoding data from the TARA Ocean expeditions highlighted the broad distribution and abundance of these two amoebozoa families (See Figure S1a,b), with Vannellidae and Paramoebidae representing respectively 53% and 39% of all the Amoebozoa 18S sequences detected in the worldwide marine waters (See Figure S1c) (Vernette et al. 2021). In line with these data, by performing a sampling along three contrasted sites along the Mediterranean coast (Sète, Banyuls and Thau) we showed that FLA belonging to the Paramoebidae and Vannellidae families are common in Mediterranean coastal waters, but Paramoebidae are significantly associated with the sediments and Vannellidae are significantly associated with the water column (Robino et al. 2025). The Paramoebidae family includes the genera *Paramoeba*, *Korotnevella*, *Neoparamoeba* and *Pseudoparamoeba* (Kudryavtsev et al. 2011). Despite their prevalence, natural associations between Paramoebidae and vibrios—and most generally bacteria—remain largely overlooked except for a recent description of an association between *Neoparamoeba perurans*—the etiological agent of the amoebic gill disease—and an uncharacterized vibrio (MacPhail et al. 2021). Given the environmental prevalence of Paramoebidae in marine environments, particularly in the sediments, and considering that the sediments were shown to represent a reservoir for some pathogenic vibrios (Lopez-Joven et al. 2018), this prompted us to investigate Paramoebidae–vibrios associations.

The present study aimed to decipher to what extent Paramoebidae can represent an intracellular niche for vibrios with pathogenic potential. By investigating different Paramoebidae isolates, we identified a natural association between the amoeba *Paramoeba atlantica* and a vibrio from the species *Vibrio bathopelagicus* that belongs to the Splendidus clade. We conducted a detailed study of the entire dynamics of interaction between *V. bathopelagicus* and *P. atlantica* at the cellular level using videomicroscopy. In addition to the characterisation of the amoeba-resistance phenotype of *V. bathopelagicus*, its virulence potential for oysters was assessed using in vivo experiments and haemocytes cytotoxicity assays. Finally, we provided evidence suggesting frequent associations between Paramoebidae and vibrios.

2 | Experimental Procedures

2.1 | Strains and Culture Conditions

All vibrio strains used in this study (See Supporting Information Material and Methods, Table S1) were grown at 20°C in LB medium, adjusted to 0.5 M NaCl (30 g·L^{-1}) unless specified otherwise. When necessary, antibiotics were added (Chloramphenicol 10 μg·mL^{-1} or Trimethoprim 10 μg·mL^{-1} for strains carrying the pMRB or the pFD086 plasmid respectively). All *Escherichia coli* strains (Supporting Information Materiel and Methods, Table S1) used in this study were cultivated in LB at 37°C, supplemented when necessary with diaminopimelic acid (DAP) 0.3 mM and Chloramphenicol 10 μg·mL^{-1} (strain carrying the pMRB plasmid). *Paramoeba atlantica* strain CCAP1560/9 was purchased from the CCAP collection (Culture Collection of Algae and Protozoa, Scotland) and was grown at 20°C in 3 mL of 70% Sterile Seawater (SSW) supplemented with 200 μL of an *Escherichia coli* SBS363 suspension (OD_{600} = 20) once a week (as a food source).

2.2 | Vibrios Isolation From *Paramoeba atlantica* Culture

Three millilitres of amoeba culture at 1–3 × 10^5 cells·mL^{-1} were resuspended in 1 mL of 70% SSW and centrifuged (1 min, 2000 g, 20°C). The pellet was resuspended in 250 μL of 70% SSW and amoeba were lysed by syringing back and forth. The lysate (100 μL) was plated on CHROMagar Vibrio (Paris, France) and incubated at 20°C for 2 days. Four colonies were selected and cryoconserved at −80°C in 20% glycerol stocks.

2.3 | Shotgun Sequencing of *P. atlantica*-Associated Microorganisms

To concentrate the *P. atlantica*-associated bacterial fraction, trophozoites of *Paramoeba atlantica* were collected, lysed using glass beads and vortexed at full speed for 2 min. After a centrifugation at 300 g for 2 min to pellet large cell debris, the supernatant was filtered through a 5 μm cellulosic membrane, allowing for the sorting out of the remaining amoeba cell debris, separating them from bacteria. The eluate was centrifuged at 5000 g for 15 min, and the pellet was used for DNA extraction using the Qiagen Blood and Tissue kit. The resulting DNA was used to prepare a library for high throughput sequencing on an Illumina MiSeq for 2 × 300 cycles. Raw reads were extracted, trimmed (Q > 30) and quality controlled using TRIMMOMATIC (version 0.38) (Bolger et al. 2014) and FASTQC (version 0.11.9). An initial assembly was performed de novo, using SPADES (version 3.12.0) with default parameters for multi cell mode (Bankevich et al. 2012). Because the sample was considered a low complexity metagenome, a manual binning approach was undertaken, using ANVI'O (version 5.3) (Eren et al. 2015). The manual curation of the obtained bins resulted in 7 bins, among which 2 corresponded in fact to two circular chromosomes of a yet undetermined Vibrio species. This metagenome-assembled genome was extracted and further explored. The sequencing data has been deposited at the NCBI under the BioProject ID PRJNA1219511.

2.4 | Vibrios Whole-Genome Sequencing and Taxonomic Assignation

Genome sequencing of *P. atlantica*-associated vibrio was performed using a combination of short- and long-read sequencing technologies. For Illumina sequencing, DNA was extracted using the NucleoSpin Tissue Kit (Macherey-Nagel) according to the manufacturer's guidelines. Paired-end reads of 150 bp were produced on the Illumina NextSeq 550 platform (Bio Environnement, Perpignan, France). For Oxford Nanopore Technologies (ONT) sequencing, DNA was extracted using the Gentra PureGene Yeast/Bacteria Kit (Qiagen) according to the manufacturer's instructions. The library was prepared using the rapid barcoding kit, and loaded on an R 9.4.1 flow cell. Sequencing was performed in high accuracy mode, and base calling was done using GUPPY (version 6.1.2) with a Qscore threshold of 9. Sequencing was performed on a MinION Mk1C device (EBI laboratory, Poitiers, France). The sequencing data have been deposited at the NCBI under the BioProject ID PRJEB83724.

For Illumina data, low-quality bases at the 3′ end of reads with a Phred quality score below 30 were removed using TRIMMOMATIC (version 0.39) (Bolger et al. 2014). The quality of the trimmed reads was assessed using FASTQC (version 0.12.1). Illumina and ONT reads were de-novo assembled using SPADES (version 3.13.1) (Bankevich et al. 2012) and the UNICYCLER pipeline (version 0.5.0) (Wick et al. 2017). Assembly quality was evaluated with QUAST (version 5.2.0) (Gurevich et al. 2013), genome completeness was assessed with BUSCO (version 5.5.0) (Simão et al. 2015) using the vibrionales_odb10 database, and genome contamination was checked with CHECKM lineage_wf (version 1.2.0) (Parks et al. 2015). Mean coverage was estimated using SAMTOOLS COVERAGE (version 1.15.1). Structural and functional genome annotation were performed by the Microscope platform (Evry, France). The sequencing data has been deposited at the NCBI under the BioProject ID PRJEB83724.

For taxonomic assignment, pairwise Average Nucleotide Identity (ANI) percentages were calculated with FASTANI (version 1.3) (Goris et al. 2007). Phylogenetic characterisation was performed using a core genome alignment of the isolated vibrio and reference strains generated with ROARY (version 3.13.0) (Page et al. 2015). Core-genome alignment was used to infer a maximum likelihood phylogeny tree with IQTREE (version 2.1.2) (Minh et al. 2020) using Ultrafast Bootstrap with 1000 bootstrap replicates (Hoang et al. 2018) and ModelFinder (Kalyaanamoorthy et al. 2017). The final phylogenetic tree was depicted using iTOL (Interactive Tree Of Life, version 6) (Letunic and Bork 2024).

2.5 | Animals-Specific Pathogen Free (SPF) Oysters

For experimental infection, juvenile *Magallana gigas* oyster batches (1.5–2 cm) were produced in 2022, in Ifremer hatchery in Argenton (Bretagne, France) from wild seed broodstocks and maintained under controlled biosecured conditions in Bouin nursery (Vendée, France) with filtered and UV-treated seawater enriched in phytoplankton (*Skeletonema costatum, Isochrysis galbana*, and *Tetraselmis suecica*) as described previously (De Lorgeril et al. 2018). For cytotoxicity evaluation, adult oysters (> 1 year old), produced in similar conditions in 2021, were used. Oysters were observed to remain free of any abnormal mortality until use.

2.6 | Vibrios and *P. atlantica* qPCR Detection

Detection of *V. bathopelagicus* DNA was performed using a *V. bathopelagicus*-specific quantitative PCR using in-house batho223-F and batho289-R primers (targeting a putative quercetin 2,3-dioxygenase) at a final concentration of 0.3 μM (Supporting Information Material and Methods, Table S2) on boiled colonies. Amplification reactions were carried out in duplicate, in a total volume of 20 μL on Mx3005 Thermocyclers (Agilent) using Brilliant III Ultra-Fast SyberGreen Master Mix (Agilent). Specificity of the amplification was estimated in silico using Primer-BLAST (Ye et al. 2012) and validated experimentally using DNA extracts from *V. harveyi, V.*

aestuarianus, V. coralliirubri, V. tasmaniensis, and V. crassostreae. Detection and quantification of *P. atlantica* DNA was performed using a *P. atlantica*-specific quantitative PCR targeting a *P. atlantica* specific region of the 18S rDNA gene (Para-atl1490-F and Para-atl1786-R primers) (Supporting Information Material and Methods, Table S2) at 0.3 μM on purified DNA under the same qPCR conditions as described above. Specificity of the amplification was estimated in silico by aligning with available *Paramoeba* 18S rRNA gene sequences (*P. eilhardi* JN202441.1, JN202440.1, JN202439.1, *P. invadens* KC790387.1, KC790386.1, KC790385.1, KC790384.1, *P. perurans* MG679920.1 and *P. aestuarina* MF197367.1, MF197366.1). Detection and quantification of GFP-expressing *V. bathopelagicus* was performed using GFP522-F and GFP625-R primers (Supporting Information Material and Methods, Table S2) at 0.3 μM under the same qPCR conditions as described above. Detection of Vibrionaceae in amoebae DNA extract from the Vibram collection (Robino et al. 2025) was performed using Vibrio567-F and Vibrio680-R primers (Supporting Information Material and Methods, Table S2). qPCR amplification reactions were performed in duplicate, in a total volume of 3 μL with Brilliant III Ultrafast Stratagene master mix, and primers at 0.2 μM, using a Roche LightCycler 480 Real-Time thermocycler (qPHD-Montpellier GenomiX platform, Montpellier University). Absolute quantification of Vibrio genomes in amoebae samples was estimated using standards from 10^1 to 10^7 genome copies of Vibrio. Only the samples containing at least 10^4 equivalents of vibrio/mL were considered positive.

2.7 | Experimental Infections

The virulence potential was estimated in vivo following a previously described procedure (Rubio et al. 2019). *V. bathopelagicus* strains (Supporting Information Material and Methods, Table S1) were grown under shaking at 20°C for 18 h in LB-NaCl. Bacteria were washed in sterile artificial seawater (SASW; NaCl 0.4 M, KCl 20 mM, $MgSO_4 + 7H_20$ 5 mM, $CaCl_2 + 2H_2O$ 1.35 mM) and adjusted to an OD_{600nm} of 1. Bacterial suspensions purity and concentration were verified by plating on LB-NaCl agar. For each condition, 100 μL of the suspension was injected intramuscularly (1.5×10^8 CFU per animal) into 30 specific pathogen-free (SPF) oysters, anaesthetised for 3 h in a hexahydrate $MgCl_2$ bath (50 g·L^{-1}, 100 oysters/L) prior to the experiment. An injection with sterile filtered seawater was used as a negative control (sham injection). After injection, animals were transferred to aquaria (10 oysters per aquarium) containing 1 L of aerated seawater at 20°C and maintained under static conditions. Mortalities were recorded at 48 h post-injection across three independent experiments. Statistical analyses were conducted using the non-parametric Kruskal-Wallis test followed by Dunn's post hoc test with Benjamini-Hochberg adjustment. Haemolymph samples from moribund oysters (2 individuals per strain of *V. bathopelagicus*) were plated after dilution. Predominant morphotypes were identified using *V. bathopelagicus*-specific qPCR using batho223-F and batho289-R primers after colony boiling in 200 μL of water. All experimental infections were performed according to the Ifremer animal care guidelines and policy.

2.8 | Cytotoxicity Assays

In vitro cytotoxicity assays were carried out according to the previously described procedure (Rubio et al. 2019). Haemocytes were plated on 96-well plates at a density of 2.10^5 cells/well. After 1 h, plasma was removed from the plate and replaced by 5 μM Sytox green diluted in 200 μL of SASW. Stationary phase bacterial suspensions (18 h at 20°C under shaking) were washed in SASW, opsonized in plasma for 30 min, and added to each well at a multiplicity of infection (MOI) of 100:1. Sytox fluorescence was measured after 16 h using a TECAN microplate reader ($\lambda_{exc} = 480$ nm; $\lambda_{em} = 550$ nm). Maximum cytotoxicity was determined by adding 0.1% Triton X-100 to haemocytes. Statistical analysis was performed using the Shapiro–Wilk test to assess the normality of the data and a Bartlett test to evaluate the homogeneity of variances. Subsequently, an ANOVA test was conducted along with a Tukey post hoc test.

2.9 | Fluorescence Microscopy

To monitor the life cycle of *V. bathopelagicus* in *P. atlantica*, amoebae were infected with a stationary phase culture of *V. bathopelagicus* GFP (18 h at 20°C under shaking) washed in 70% SSW prior to the experiment. The infection was conducted at a MOI of 1000:1 in a 96-well microplate (PS μclear Chimney Well, Greiner Bio-one) with 3×10^4 amoebae per well in 70% SSW. The microplate was centrifuged at 400 g for 5 min at 20°C to synchronise the phagocytosis before being incubated statically at 20°C. Fluorescence microscopy imaging was carried out from 30 min to 24 h post-exposure to the bacteria using an Axio Vert.A1 microscope with an Axiocam 208 colour camera (for real-time imaging) and an Axio Observer microscope with an AxioCam 503 mono camera (for time-lapse imaging) (Zeiss, Feldbach, Switzerland). For time-lapse imaging, pictures were taken every minute in a single field. Extracellular bacteria were removed by washing with 70% SSW prior to microscopic acquisitions. The proportion of amoebae with a vacuole containing motile GFP-expressing bacteria was quantified after 24 h of incubation using real-time video microscopy acquisitions.

2.10 | Confocal Laser Scanning Imaging

Confocal laser scanning microscopy images were obtained using an inverted Zeiss LSM880 confocal microscope (Zeiss, Feldbach, Switzerland). For time-lapse imaging, images were captured every second in a single plane. Experiments were conducted in Fluorodish (World Precision Instrument) at a cell density of 4.5×10^5 amoeba per Fluorodish. Phagocytosis was synchronised by centrifugation as described before.

To determine if *V. bathopelagicus* remains in phagosomal compartments during the course of an infection, amoebae were fed one-micrometre Fluoresbrite Bright Blue (BB) microspheres (Polysciences Inc., Eppelheim, Germany). Amoebae were either exposed simultaneously to the beads (MOI 500:1) and the vibrios (MOI 1000:1) or subjected to a pulse-chase experiment, where amoebae were first exposed to the beads for 1.5 h

(MOI 500:1) followed by exposure to the vibrios for 2.5 h (MOI 1000:1). Fluorodish was washed with SSW 70% prior to confocal acquisition.

To monitor the survival of *V. bathopelagicus* in acid conditions, amoebae media was supplemented with 25 μg·mL^{-1} pHrodo Red Dextran 10,000 MW (Molecular probes) and amoebae were exposed to *V. bathopelagicus* Sal10 GFP for 1 h or 4 h in a Fluorodish. After these treatments, extracellular vibrios were removed, and imaging was performed using a confocal microscope as described previously.

To determine whether the vibrio load in the vacuole is clonal, amoebae were exposed simultaneously to *V. bathopelagicus* Sal10 GFP and mCherry at a ratio of 1:1 (final MOI of 1000:1) for 4 h. In a separate pulse-chase experiment, amoebae were initially exposed to *V. bathopelagicus* Sal10 GFP (MOI 1000:1) for 0.5 h followed by exposure to *V. bathopelagicus* mCherry for 3.5 h (MOI 1000:1).

2.11 | Measuring Vibrio and Amoeba Abundance Over Time in Co-Culture

To monitor the evolution of vibrio and amoeba populations during their interaction, their loads were quantified by qPCR during the course of an interaction over a 7-day period. Amoebae were infected with a stationary-phase culture of *Vibrio bathopelagicus* Sal10 GFP (grown for 18 h at 20°C with shaking) and washed in 70% SSW prior to the experiment. The infection was performed at a multiplicity of infection (MOI) of 1000:1 in a 96-well microplate (PS μclear Chimney Well, Greiner Bio-One) as described above (see Section 2.9). At specific time points (0, 2, 4, 6, 8, 24, 48 and 168 h), the total well contents were scraped, and DNA was extracted using the NucleoSpin Tissue Kit (Macherey-Nagel). Vibrio and amoeba loads were quantified by qPCR using the primer pairs GFP522-F/GFP625-R and Para-atl1490-F/Para-atl1786-R, respectively (Supporting Information Material and Methods, Table S2). As control conditions, amoebae were fed *E. coli* SBS363 at an MOI equivalent to that used for vibrios, and vibrios were also incubated in 70% SSW without amoebae. Statistical comparison of the relative fitness of vibrios in the presence or absence of the amoebae at each time point was performed using a Welch t-test following a Shapiro–Wilk test to assess normality.

3 | Results

3.1 | *Paramoeba atlantica* CCAP 1560/9 Is Stably Associated With *Vibrio bathopelagicus*

To identify ecologically realistic Paramoebidae-Vibrio interaction systems, different amoebal cultures available from the CCAP collection were initially screened using a 16S rRNA gene Vibrionaceae specific qPCR. Although isolates *Pseudoparamoeba pagei* 1566/1 and *Neoparamoeba pemaquidensis* 1560/4 tested negative, the presence of Vibrio was detected in *Paramoeba atlantica* 1560/9, in accordance with previous detection of Vibrio sequences in metagenomic analysis of this culture (BioProject ID: PRJNA1219511).

To isolate the Vibrio strain(s) associated with *P. atlantica* 1560/9 detected within the metagenomic data and the 16S specific qPCR, a new independent culture was ordered from the CCAP and the amoeba lysate was plated on vibrio-selective culture media (CHROMagar Vibrio). Four isolated colonies were randomly picked and selected for whole-genome sequencing of the *P. atlantica*-associated vibrios (Bioproject ID: PRJEB83724, Table S1). Genome assembly and ANI (Average Nucleotide Identity) score calculations confirmed the clonality of the isolated vibrios (ANI > 99.98%; Table S2). Long-read sequencing data, obtained with a Nanopore MinION sequencer, and Illumina data were combined (Bioproject ID: PRJEB83724). The resulting hybrid assembly enabled the reconstitution of two circular chromosomes of 3,452,054 bp and 2,023,251 bp with a GC% of 44.08% (See Table S1) (Bioproject ID: PRJEB83724). Following these results, we compared the *gyrB*, *rctB*, and *topA* genes from the metagenomic and whole-genome sequencing data, obtained 2 years apart, which showed 100% nucleotide identity, highlighting the stability of this association.

From a taxonomic perspective, ANI analyses identified that this strain, hereafter named Pa22, belongs to *V. bathopelagicus* (97.89% ANI; Table S2). This species, recently described, currently includes only one other strain named Sal10 (Lasa et al. 2021). Phylogenomic analyses, based on the alignment of 130 concatenated gene sequences, confirmed that Pa22 belongs to the Splendidus clade (Figure 1).

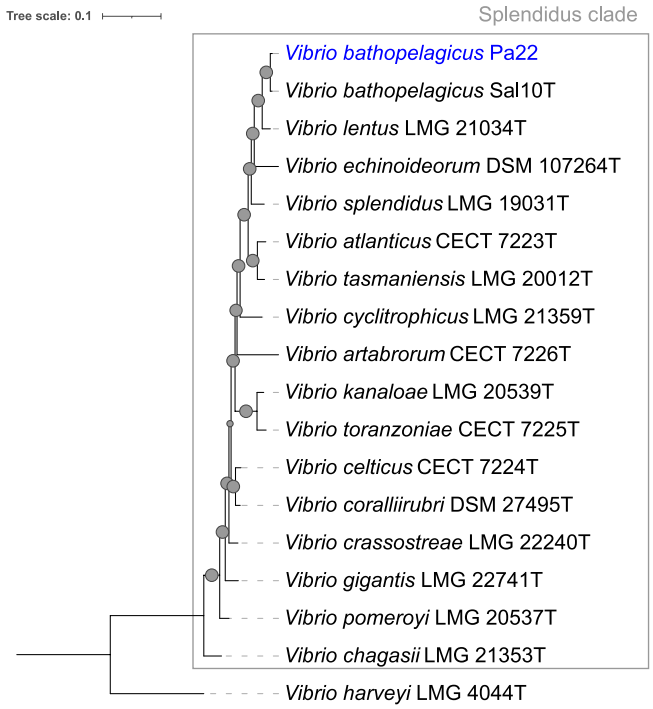

FIGURE 1 | *Vibrio bathopelagicus* Pa22 belongs to the Splendidus clade. Maximum likelihood phylogenetic tree calculated with IQ-TREE from nucleotide alignments (104,067 nucleotides sites) of the core genome (130 core genes with 95% minimal identity for BLASTp) (GTR + F + R7 substitution model). Bootstrap values (1000 replications) are represented by circles proportional to their value (from 57% to 100%). The scale bar represents the number of nucleotide substitutions per site. *V. harveyi* LMG4044T was used as an outgroup in the analysis.

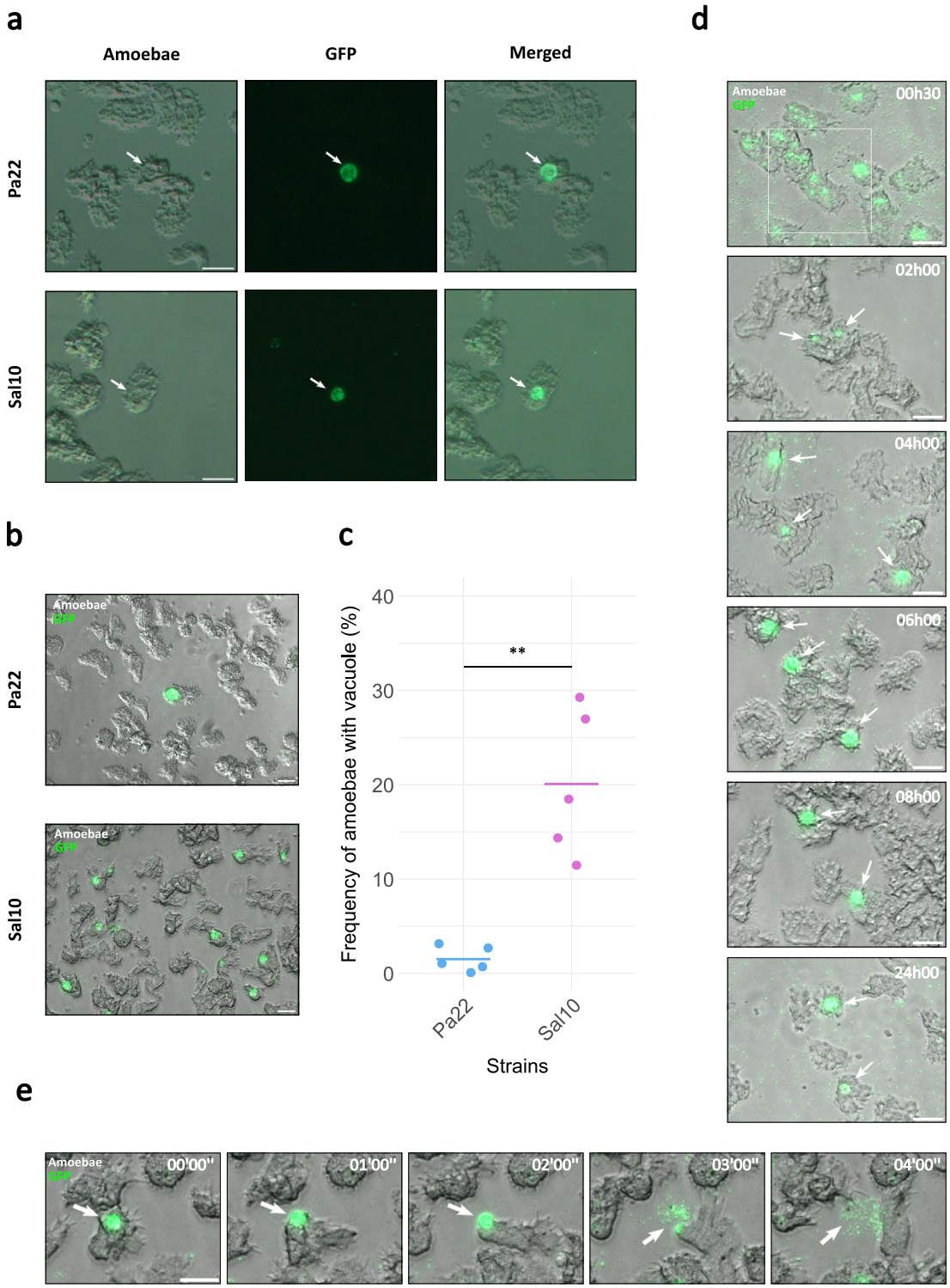

FIGURE 2 | Legend on next page.

3.2 | *V. bathopelagicus* Persists Within a Large Vacuole in *P. atlantica* Before Its Extracellular Release via Exocytosis

To investigate the mechanisms enabling *V. bathopelagicus* Pa22 to persist with *P. atlantica*, we studied the interaction at a cellular level using real-time and time-lapse imaging and videomicroscopy. Within *P. atlantica* culture, some amoebae exhibited large vacuoles filled with motile bacteria (Video S1). To determine whether the associated vibrio can colonise and persist within this intracellular structure, *P. atlantica* were exposed to a GFP-expressing strain of *V. bathopelagicus* Pa22 for 24 h prior to imaging. Consistent with our initial observation in the untreated culture (Video S1), some amoebae displayed a unique large vacuole colonised by motile GFP-vibrios (Figure 2a and Video S2). Motility and strong expression of GFP indicated that internalised *V. bathopelagicus* remains alive. To determine whether this phenotype is specific to the Pa22 strain or conserved in the *V. bathopelagicus* species, we exposed *P.*

FIGURE 2 | *V. bathopelagicus* remains viable within a large vacuole in *P. atlantica* before its extracellular release by exocytosis. (a) *V. bathopelagicus* strain Pa22 GFP and Sal10 GFP can colonise a large vacuole within *P. atlantica* while retaining their motility and viability. Amoebae are visible in the light-transmitted channel (labelled Amoebae) and GFP-expressing bacteria are visible in the green channel (labelled GFP). Merged images are shown on the right. Images were captured after 24 h of interaction using Hoffman contrast microscopy (See Videos S2 and S3). The white arrow indicates the vacuole containing motile vibrios. Scale bar: 30 μm. (b) Merged images illustrating the strain-dependency of vacuoles formation frequency. Amoebae are visible in the light-transmitted channel and vibrios in the green channel. Images were taken after 24 h of interaction using fluorescence phase-contrast microscopy. (c) The frequency of vacuole apparition in amoebae is significantly higher when exposed to *V. bathopelagicus* Sal10 GFP compared to *V. bathopelagicus* Pa22 GFP after 24 h of interaction. Each dot represents an independent experiment in which at least 140 cells were counted. (**: p-value < 0.01, Welch t-test). The bar indicates the mean vacuole formation frequency across the 5 independents experiments. (d) Kinetics of the interaction between *P. atlantica* and *V. bathopelagicus* Sal10 GFP. Time-lapse images from fluorescence phase contrast microscopy. Images were taken from 0.5 to 24 h of interaction (the time post-exposure is indicated on each image on the upper right corner). Image composition is as described in Figure 2b. In the 0.5 h image, the white square highlights the region shown at higher magnification in Figure S2. The white arrow (from 2 to 24 h post-exposure) indicates vibrios contained in a single vacuole per amoebae. Scale bar 30 μM. (e) Time-lapse images from fluorescence phase-contrast microscopy showing the release of live *V. bathopelagicus* Sal10 GFP into the extracellular medium via exocytosis. Image were acquired after 24 h of interaction during 4 min (relative time is shown on the upper right corner). Image composition is as described for Figure 2b. Scale bar: 30 μm.

atlantica to a GFP-expressing Sal10 strain, the only other known species member. Similar to Pa22, after 24 h of interaction with Sal10, some amoebae exhibited large vacuoles containing motile GFP-vibrio (Figure 2a and Video S3).

To assess the frequency of vacuole colonisation for each strain of *V. bathopelagicus*, we quantified the percentage of amoebae containing a vacuole filled with motile bacteria after 24 h of interaction with GFP-expressing vibrios. The percentage of amoebae with vacuoles colonised by motile vibrios varied by strain, with 20% of amoebae exposed to GFP-Sal10 containing a vacuole, compared to only 1.7% for those exposed to GFP-Pa22 (p-value < 0.01, Welch t-test) (Figure 2b,c).

To better understand the life cycle of *V. bathopelagicus* within *P. atlantica*, we monitored the interaction kinetics by phase contrast fluorescence microscopy. Given the higher frequency of vacuole colonisation with Sal10, this strain was selected over Pa22 to further study the cellular mechanisms of this interaction. Microscopy images were captured at various time points up to 24 h post infection of *P. atlantica* by GFP-Sal10. After 30 min of interaction, we observed a strong phagocytosis with intracellular vibrios contained in multiple phagosomes per amoeba (Figure 2d and Figure S2). Within the first 2 h, a rapid decrease of GFP fluorescence intensity in these phagosomes was detected, indicating bacterial killing and degradation (Video S4 and Figure S3). Despite this initial digestion, motile and viable intracellular vibrios were detectable from 2 h up to 24 h after the initial interaction within a single large vacuole per amoeba.

As early as 4 h post infection, *V. bathopelagicus* can be expelled from *P. atlantica* by exocytosis, resulting in the egress of live and highly motile vibrios into the extracellular environment (Figure 2e and Video S5). This event is non-lytic for the amoeba, which exhibited normal morphology and behaviour post-exocytosis (Video S5).

3.3 | *V. bathopelagicus* Remains in the Phagosomal Compartment

For some bacteria, resistance to digestion during phagosome maturation relies on their ability to escape from phagosomal compartments, either to the cytosol or into other non-bactericidal cellular compartments (Hagedorn and Soldati 2007; Schulz et al. 2014; Van der Henst et al. 2016). To determine whether *V. bathopelagicus* remains in the endophagosomal compartment, *P. atlantica* was simultaneously exposed to *V. bathopelagicus* GFP-Sal10 and fluorescent indigestible beads (diameter of 1 μm), used as a tracker of the phagosomal compartment. After 4 h of interaction, the presence of beads within vacuoles that also contained motile vibrios could be observed (Figure 3a). To confirm that the beads were not co-transported into this cellular structure via vibrios-containing phagosomes, a pulse-chase experiment was conducted in which *P. atlantica*'s digestive tract was pre-loaded with fluorescent beads for 1.5 h before exposure to GFP-Sal10 for 2.5 h. Consistently, motile vibrios were found in vacuoles pre-loaded with beads (Figure 3a). This indicates that the vibrios colonise and remain in a vacuole that belongs to the phagosomal compartment.

To further investigate whether *V. bathopelagicus* viability is affected by the acidification of this digestive compartment, amoebae were exposed to GFP-Sal10 in the presence of pHrodo-Dextran, a pH sensitive fluorescent dye-conjugated polysaccharide whose fluorescence increases as the pH becomes more acidic. After 4 h of interaction, confocal imaging revealed that the vibrio-containing vacuoles (VCV) were acidified after a contact with an acidic lysosomal compartment (Figure 3b). Acidified vibrio-containing compartments were observed after 1 h of exposure (Figure 3c) as well as after 4 h (Figure 3c). Remarkably, the vibrios maintained their motility even in acidified vacuoles (see Video S6). These results indicate that *V. bathopelagicus* does not only tolerate the acidification but also remains viable within this hostile, acidic environment of the amoeba's phagosomal compartment. This is further supported by the fact that the pH threshold for growth of both *V. bathopelagicus* strains lies between pH 4 and pH 5 in vitro (Figure S4).

In amoeba, the final step of phagocytosis involves the retrieval of the V-ATPases from the phagolysosome, which results in an increase in the phagolysosome pH, giving rise to a cellular compartment called the post-lysosome. Ultimately, amoeba expel undigested residues via exocytosis (Dunn et al. 2018). Consistent with this process, we observed that the VCV can be neutralised

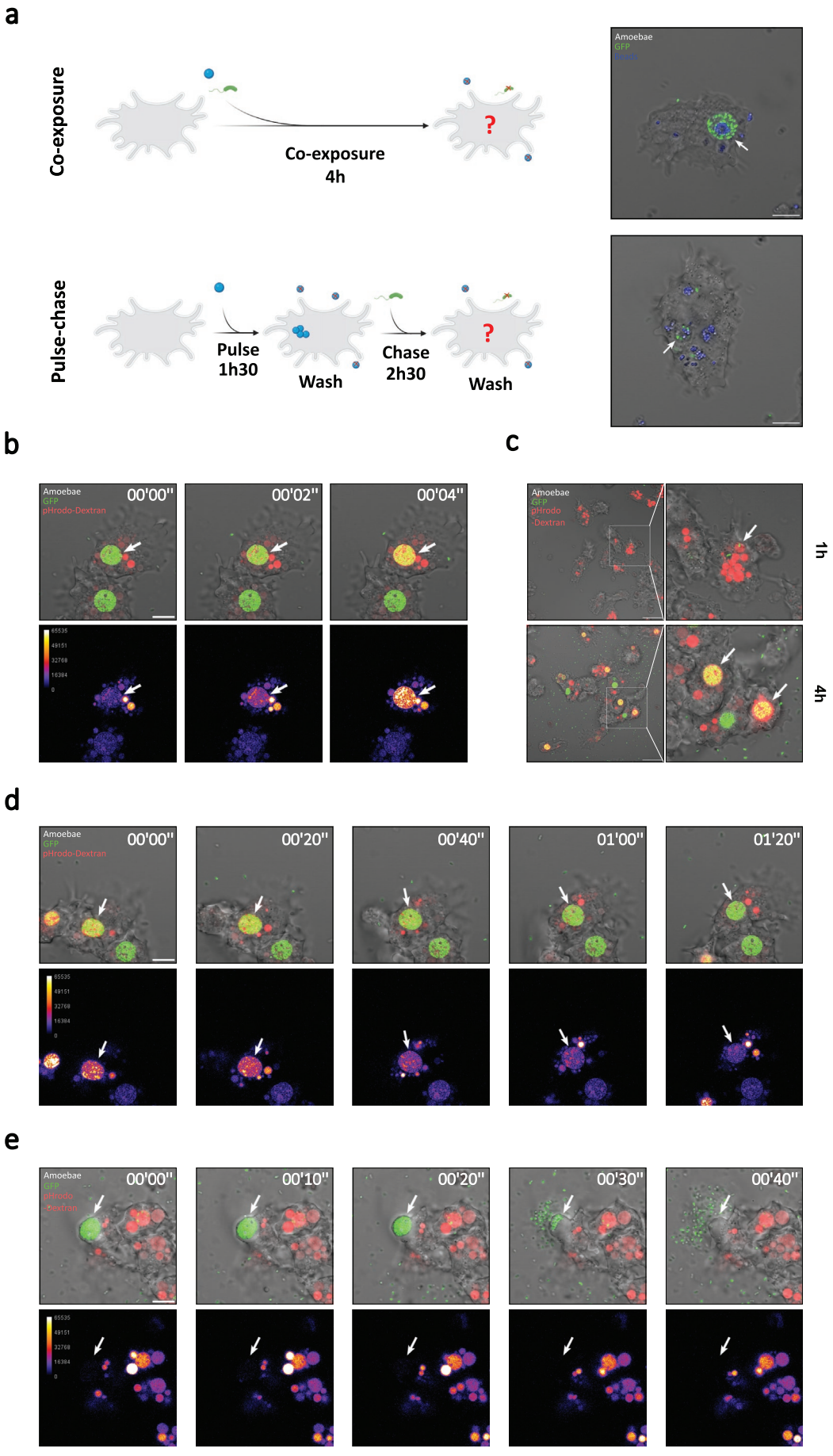

FIGURE 3 | Legend on next page.

FIGURE 3 | *V. bathopelagicus* undergoes a complete phagocytic cycle before release. (a) Confocal laser scanning microscopy (CLSM) images of amoebae (light-transmitted channel) exposed to non-digestible fluorescent beads (blue channel) and GFP-labelled *V. bathopelagicus* Sal10 (green channel) for 4 h (labelled 'Co-exposure'). A separate pulse-chase experiment shows amoebae exposed to beads for 1.5 h (pulse), followed by removal of extracellular beads and subsequent exposure to *V. bathopelagicus* Sal10 GFP for 2.5 h (chase) (labelled 'Pulse-chase'). For both images, the white arrow indicates the vacuole containing motile vibrios. Scale bar: 10 μm. (b) Time-lapse CLSM images illustrating the acidification of a vibrio-containing vacuole following a contact of the vacuole with an acidic compartment. Amoebae are visible in the transmitted light-channel, GFP-*V. bathopelagicus* Sal10 in the green channel and pHrodo-Dextran in the red channel (indicating acidic compartments). The FIRE lookup table (LUT) was applied to the images acquired from the red channel, specifically highlighting the signal corresponding to pHrodo-dextran. Images were acquired after 4 h of interaction during 4 s (relative time is shown on the upper right corner). The white arrow indicates the vacuole containing the vibrios. Scale bar: 10 μm. (c) CLSM images of amoeba exposed to GFP-Sal10 and pHrodo-Dextran for 1 h (upper panel) and 4 h (lower panel). The acid compartments are indicated by the white arrows. Image composition is as described for the upper panel of Figure 4b. Scale bar 10 μm. (d) Time-lapse CLSM images illustrating the neutralisation of the vibrio-containing vacuole. Images composition is as described for Figure 4b. Images were captured after 4 h of interaction during 1 min 20. Scale bar 10 μm (e) Time-lapse CLSM images reveal that the content of the digestive vacuole is neutralised before exocytosis. Images were captured after 4 h of interaction during 40 s. Image composition is as described for Figure 4b. Scale bar: 10 μm.

(Figure 3d) and that the VCV had a neutral pH just before exocytosis (Figure 3e). This suggests that the release of live vibrios occurs after a neutralisation of the vacuole, mirroring the process of expelling phagocytic waste at the end of the phagocytic cycle. These observations imply that *V. bathopelagicus* can persist within the amoeba until the end of the phagocytic cycle, ultimately being released in a non-lytic manner, with the vacuole neutralised prior to exocytosis.

3.4 | *V. bathopelagicus* Can Multiply Within *P. atlantica* Without Interfering With the Amoebae Fitness

Confocal imaging revealed a progressive increase in bacterial density within the vibrio-containing vacuole (VCV) during the course of the interaction with a notable accumulation of vibrios by 4 h (Figure 4a) as well as an increase in vacuole size (Figure 4b). To determine whether this bacterial load arises from the clonal multiplication of a single bacterium, amoebae were exposed to a 1:1 mixture of GFP- and mCherry-Sal10. After 4 h of interaction, confocal imaging showed the presence of both GFP- and mCherry-vibrios within most VCV (14 bicolor vacuoles out of 17 observed with 2 GFP-only and 1 mCherry-only) indicating that the high vibrio density was not due to the clonal expansion of a single bacterium (Figure 4c). This finding also suggests that even if initial phagosomes contain individual bacteria, they can fuse, allowing multiple bacteria to coexist in the same compartment. Nevertheless, we also observed bacterial septa suggesting that active bacterial division can occur within the VCV (Figure 4c).

To further investigate whether the increasing bacterial load results from continuous fusion of the VCV with new phagosomes containing vibrios, pulse-chase experiments using colour-coded Sal10 vibrios were performed. Amoebae were first exposed to GFP-Sal10 for 0.5 h, followed by exposure to mCherry-Sal10 for an additional 3.5 h before imaging. Confocal microscopy revealed the exclusive presence of GFP-vibrios within the VCVs ($n = 31$ observed vacuoles), indicating that 30 min after the initial phagocytosis, the VCV is not accessible anymore for fusion with newly formed phagosomes (Figure 4d). Newly formed mCherry-Sal10 containing phagosomes could be observed in amoebae presenting GFP-Sal10 containing VCV, indicating that mCherry-Sal10 was still phagocyted (Figure S5).

To quantify the effect of *P. atlantica* on *V. bathopelagicus* population, qPCR was used to monitor vibrio load (intra- and extracellular) during an interaction. This analysis revealed a significant decrease in bacterial load within the first 2 h, followed by an increase from 2 to 8 h, eventually reaching a stable load thereafter (Figure 4e). These results are consistent with the observation of bacterial septa within VCVs observed by confocal microscopy (Figure 4c). The presence of vibrios did not result in a reduction in the amoeba population over time compared to the control condition, where amoebae were exposed to *E. coli* SBS363. This suggests that the interaction does not cause any significant damage to the amoebae, in agreement with the previous microscopic observations (Figure 4f).

Collectively, these results suggest that the vacuole initially forms through the fusion of individual phagosomes during the first hours of the interaction, followed by a phase during which the VCV becomes inaccessible for fusion with additional phagosomes and then the bacterial load increases further by intracellular replication.

3.5 | *Vibrio Bathopelagicus* Shows Potential Virulence for Oysters

Due to the phylogenetic proximity of *V. bathopelagicus* with known pathogenic strains for oysters, its virulence potential was assessed in experimental infections. The two strains, Pa22 and Sal10, exhibited high virulence potential 48 h post-injection, with mortality rates of 65% and 71.25%, respectively, compared to the seawater control and the avirulent strain *V. tasmaniensis* LMG20012T (Figure 5a). The presence of *V. bathopelagicus* Pa22 and Sal10 in diseased animals was confirmed by spreading haemolymph from moribund oysters on nutrient medium and specific qPCR of *V. bathopelagicus* on colonies, demonstrating its involvement in the observed mortalities (Henle and Marchand 1910).

Within the Splendidus clade, the virulence of oyster pathogenic vibrios mostly relies on their cytotoxicity towards haemocytes, the

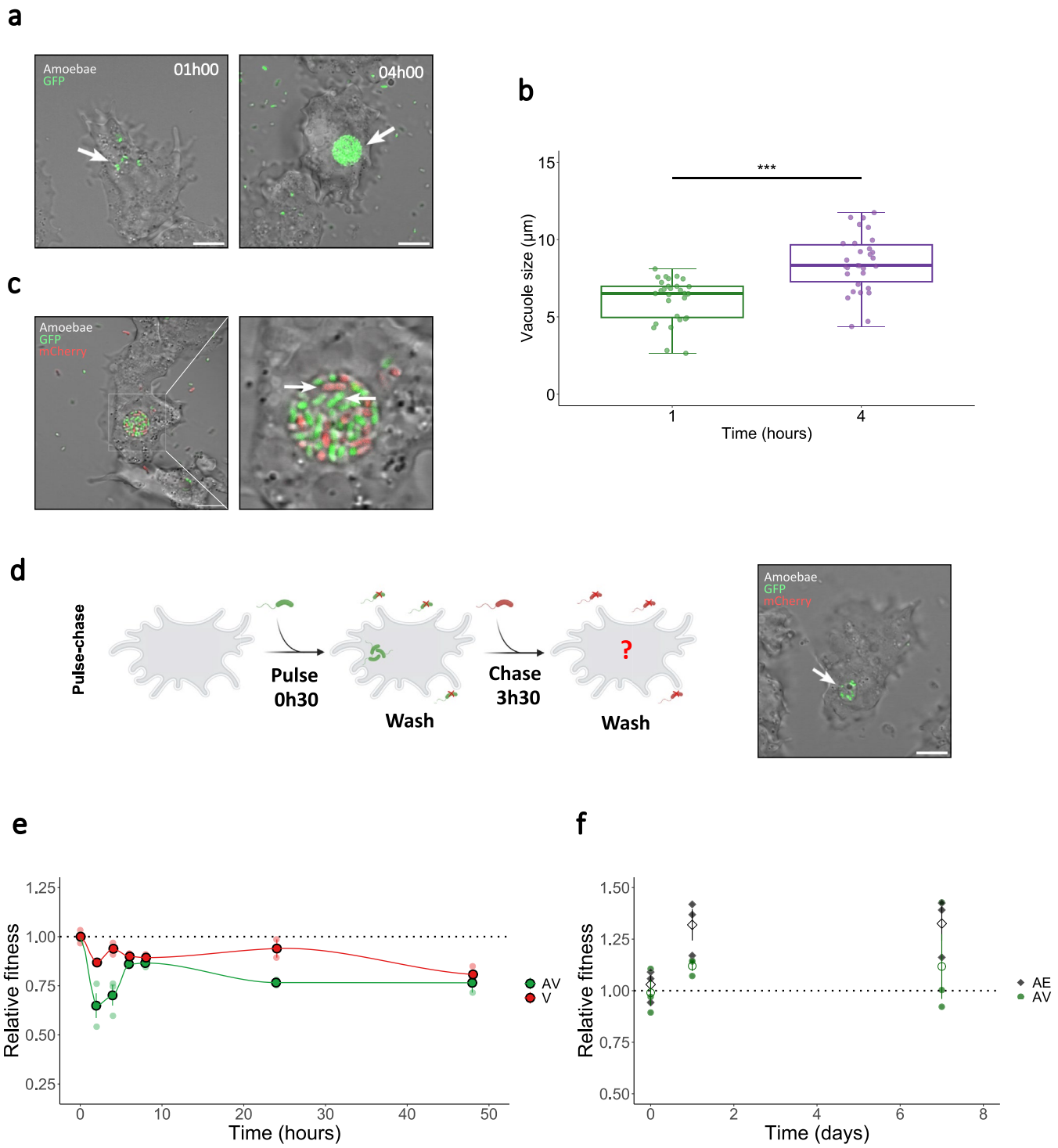

FIGURE 4 | Legend on next page.

immune cells of oysters. To determine whether *Vibrio bathopelagicus* exhibits this phenotype, a cytotoxicity assay was performed. Similar to other pathogenic vibrios of the Splendidus clade, Pa22 and Sal10 caused significant lysis of haemocytes (60%) after 16 h of infection, a result comparable to the cytotoxic effects observed with the known cytotoxic strain LGP32 (Figure 5b).

Considering the virulence phenotype in amoeba and in oyster, we looked for potential virulence factors in *V. bathopelagicus* Pa22 genome that are also described in Splendidus vibrios or in other pathogenic vibrios. This analysis revealed the presence of potential virulence genes commonly described in pathogenic Vibrio and whose biological function or involvement in virulence has been experimentally validated (Table S3). This analysis revealed the presence of virulence factors commonly described within the Splendidus clade such as the OmpU porin, the exported protein of unknown function R5.7, the vsm metalloprotease, and a Type VI Secretion system. The genome of *V. bathopelagicus Pa22* also contains the rtxACHBDE gene cluster, which encodes the MARTX toxin,

FIGURE 4 | *Vibrio bathopelagicus* can multiply within *P. atlantica* without interfering with the amoeba fitness. (a) CLSM images illustrating the increase in bacterial load within the vacuole between 1 and 4 h of interaction. Amoebae are visible in the transmitted light-channel, GFP-*V. bathopelagicus* Sal10 in the green channel. Scale bar 10 μm. (b) Increase in VCV size between 1 and 4 h of *P. atlantica*-*V. bathopelagicus* Sal10 interaction. Vacuole size was measured in 30 amoebae at 1 or 4 h post-exposure to *V. bathopelagicus* Sal10 using ImageJ. Vacuole sizes were compared between time points (***p-value <0.001, Mann–Whitney test). (c) CLSM images of amoebae simultaneously exposed to GFP (green) and mCherry (red)-labelled *V. bathopelagicus* at a ratio of 1:1 (MOI 1000:1). Images were acquired after 4 h of interaction. Bacterial septa are visible on the right image (indicated by white arrows). Scale bar 10 μm. (d) A pulse-chase experiment where *P. atlantica* was exposed to GFP-labelled bacteria for 0.5 h, then to mCherry-labelled bacteria for 3.5 h before CLSM acquisition. The white arrow indicates the vacuole containing motile vibrios. Scale bar: 10 μm. (e) Total vibrio load was evaluated by GFP-specific qPCR during the course of the interaction at 0, 2, 4, 6, 8, 24 and 48 h. At each time point, vibrio load is expressed as relative fitness, normalised to the load observed at time point J0. The 'AV' condition (green) correspond to *V. bathopelagicus* Sal10 GFP in the presence of *P. atlantica* while the 'V' condition (red) serves as the control condition, consisting solely of *V. bathopelagicus* Sal10 GFP in 70% SSW. Statistical comparison of the relative fitness of vibrios in the presence or absence of amoebae at each time point was performed using a Welch t-test, revealing significant differences at 2 h (p-value = 0.036) and at 4 h (p-value = 0.025). (f) Amoeba population dynamics were monitored throughout the interaction at days 0, 1 and 7 using *P. atlantica*-specific qPCR. At each time point, amoeba load is expressed as relative fitness, normalised to the load observed at time point J0. The 'AV' condition (green) correspond to *P. atlantica* co-cultured with *V. bathopelagicus* Sal10 GFP while the 'AE' condition (grey) serves as the control condition, consisting of *P. atlantica* fed with *E. coli* SBS363.

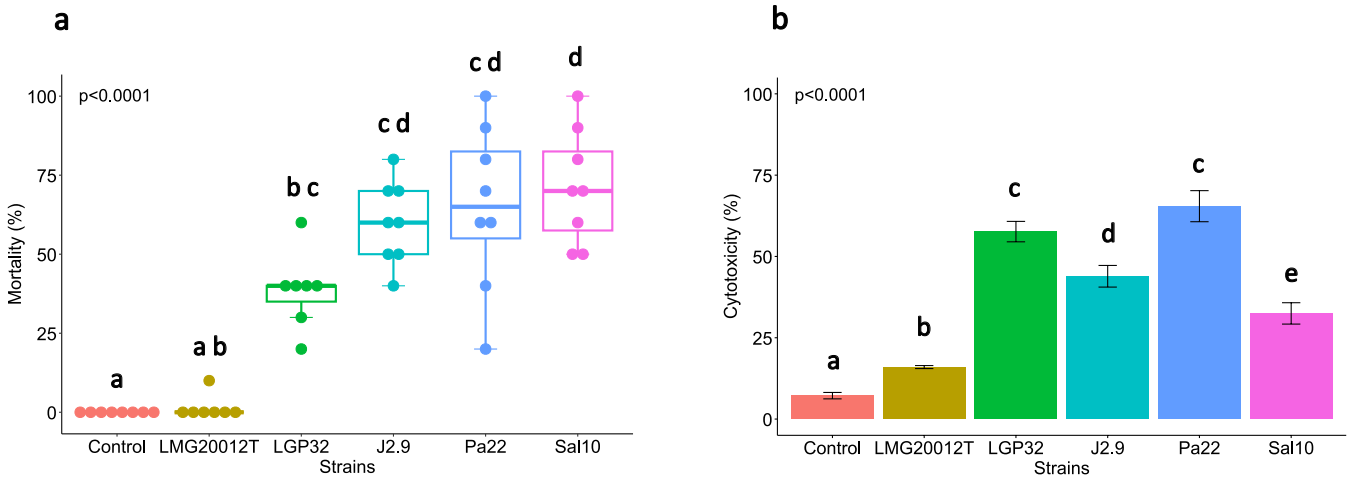

FIGURE 5 | Virulence potential and cytotoxicity of *V. bathopelagicus* strains. (a) Calibrated bacterial suspensions of strains Pa22 and Sal10 were injected into the adductor muscle of anaesthetised juvenile oysters (1.5×10^8 CFU/animal). After injection, the animals were placed in tanks of 10 animals and mortalities were measured after 48 h. As a control, artificial seawater, bacterial suspensions of virulent strains (*V. tasmaniensis* LGP32, *V. crassostreae* J2.9) and avirulent strains (*V. tasmaniensis* LMG20012T) were injected. The figure shows a significant increase in the mortality rate of oysters exposed to the two strains Sal10 (pink) and Pa22 (dark blue) compared with the artificial seawater control (red) after 48 h. Mortality rates at 48 h were compared for each vibrio strain using the Kruskal-Wallis test and a Dunn's post hoc test with Benjamini-Hochberg adjustment. Each point corresponds to a tank of 10 animals. Control ($n = 80$); Pa22 ($n = 80$), Sal10 ($n = 80$), J2.9 ($n = 80$), LGP32 ($n = 70$), LMG20012T ($n = 70$). These results come from three independent experiments. (b) Haemocytes were exposed to *V. bathopelagicus* Pa22 at an MOI of 100:1. Quantification of cell lysis was performed by measuring the fluorescence of Sytox green, a non-cell-permeable fluorescent DNA intercalant that allows quantification of extracellular DNA. The figure shows the percentage of haemocyte lysis after 16 h of exposure to *V. bathopelagicus* Pa22. *V. tasmaniensis* LGP32 and *V. bathopelagicus* Sal10 were used as positive controls. The control condition refers to basal cell lysis of haemocytes measured during the 16 h experiment. Statistical analyses were performed by first testing the assumption of normality using the Shapiro–Wilk test and the homogeneity of variances using Bartlett test. Data meeting these assumptions were subsequently analysed using ANOVA, followed by Tukey's post hoc test for multiple comparisons. The graphics illustrate the result of one experiment representative of three independent experiments.

only found for the Splendidus clade in *V. splendidus* and *V. bathopelagicus*. We also analysed differences in the virulome of Pa22 and Sal10, revealing that Sal10 possesses an additional Type VI Secretion System located on its second chromosome (Table S4). Furthermore, Pa22 and Sal10 exhibit distinct genetic repertoires for O-antigen and capsule biosynthesis, sharing some common genes while also harbouring unique loci suggesting differences in their LPS and capsule structures. (See Table S5).

3.6 | Survival Within *P. atlantica* Is Widespread Across Vibrios

To determine whether the ability to persist within a VCV is shared by other Vibrio species, we exposed *P. atlantica* to strains that are more or less phylogenetically related to V. *bathopelagicus*. These included six strains from the Splendidus clade (*V. splendidus* 4G1-8, *V. splendidus* 4G4-4, *V. tasmaniensis* LGP32, *V. tasmaniensis* LMG20012T, *V. crassostreae* J2-8,

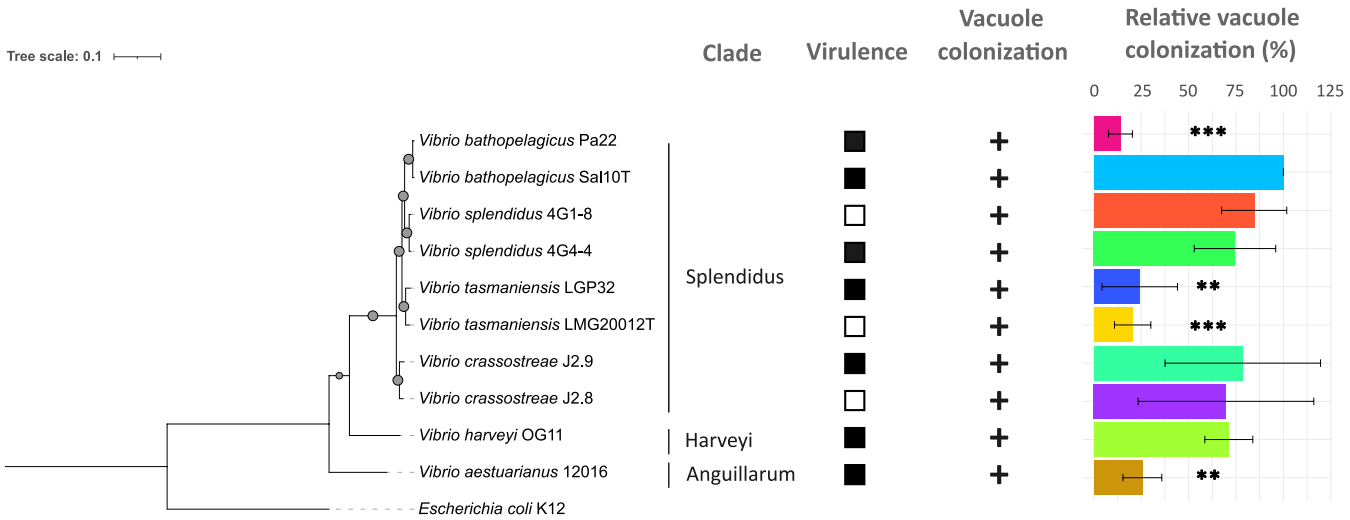

FIGURE 6 | The ability to colonise *P. atlantica* vacuole is shared among phylogenetically distant vibrios. Maximum likelihood phylogenetic tree calculated with IQ-TREE from nucleotide alignments (42,289 nucleotides sites) of the core genome (56 core genes with 85% minimal identity for BLASTp) (GTR + F + I + R2 substitution model) of the tested phylogenetically distant vibrios. Bootstrap values (1000 replications) are represented by circles proportional to their value (ranging from 54% to 100%). *Escherichia coli* K12 was used as an outgroup in the analysis. The scale bar represents the number of nucleotide substitution per site. The virulence phenotype in oyster is indicated by a black square (virulent strains) or a white square (avirulent strains) while the ability to colonise the vacuole is denoted by a '+'. The relative proportion of vacuole formation in *P. atlantica* after 24 h of exposure to each strain was determined by comparing the vacuole formation frequency of each strain to that of Sal10 (used as the reference value—set at 100%). Bar graph shows the mean relative vacuole formation frequency for each strain and the standard deviation from at least three independent experiment per strain. Statistical analysis was performed by first assessing data normality (Shapiro–Wilk test) followed by a t-test comparing the mean vacuole formation frequency of each strain to the reference value (Sal10—100%). (***p-value <0.001; **p-value <0.01).

and *V. crassostreae* J2-9), one strain from the Harveyi clade (*V. harveyi* OG11), and one strain from the Anguillarum clade (*V. aestuarianus* 12016). These strains exhibit contrasting virulence profiles in oysters, with virulent strains (*V. splendidus* 4G4-4, *V. tasmaniensis* LGP32, *V. crassostreae* J2-9, *V. harveyi* OG11, and *V. aestuarianus* 12016) and avirulent strains (*V. splendidus* 4G1-8, *V. tasmaniensis* LMG20012T, and *V. crassostreae* J2-8). All tested Vibrio strains were able to persist and maintain motility within *P. atlantica*, residing in large vacuoles similar to those observed with *V. bathopelagicus*. Interestingly, the frequency of vacuole formation varied significantly among strains, independently of their virulence profiles. The highest frequencies were observed with *V. splendidus* and *V. crassostreae* strains, as well as with *V. harveyi* OG11 (Figure 6).

3.7 | Vibrios Are Frequently Associated With Paramoebidae in Marine Environment

To assess the frequency of Vibrio-Paramoebidae associations, we screened amoeba DNA from the Vibram collection using Vibrionaceae-specific qPCR. The Vibram collection comes from an extensive survey of amoebae diversity in Mediterranean environments (Supporting Information Material and Methods). Over the course of a year, monthly samples were collected across three compartments—water column, sediments, and oysters—across three sites with varying levels of anthropogenic influence. This collection includes Paramoebidae, Vannellidae, Acanthamoebidae, and Vexiliferae amoebae as well as unassigned taxa. Our results revealed an association between vibrios and every amoeba family (Figure 7). Interestingly, Paramoebidae were frequently associated with vibrios—with 45 amoebae out of 76 screened amoebae—indicating that vibrio and Paramoebidae frequently encounter each other in the environment, further reinforcing the ecological significance of this interaction.

4 | Discussion

Several studies involving model organisms and experimental cocultures suggested that amoebae may serve as environmental reservoirs for pathogenic vibrios, promoting their persistence, dissemination and/or multiplication (Van der Henst et al. 2016, 2018; Sandström et al. 2010; Laskowski-Arce and Orth 2008). However, despite the prevalence and genetic diversity of both amoebae and vibrios, the characteristics and extent of their associations in natural environments—particularly in marine ecosystems—remain largely unexplored. In this work, we described a natural interaction between *P. atlantica*, a marine environmental amoeba, and its associated vibrio from the species *V. bathopelagicus*, and we investigated the cellular mechanisms underlying this association. We demonstrated that *V. bathopelagicus* can survive and multiply intracellularly within the amoeba before being expelled, potentially contributing to its environmental persistence and dissemination. Interestingly, this trait is not unique to *V. bathopelagicus*, as a similar phenotype has been observed with distantly related vibrio strains.

We observed that *Vibrio bathopelagicus* can survive *P. atlantica* digestion and persist intracellularly within a single large vacuole per amoeba, which we named the VCV. The co-localization

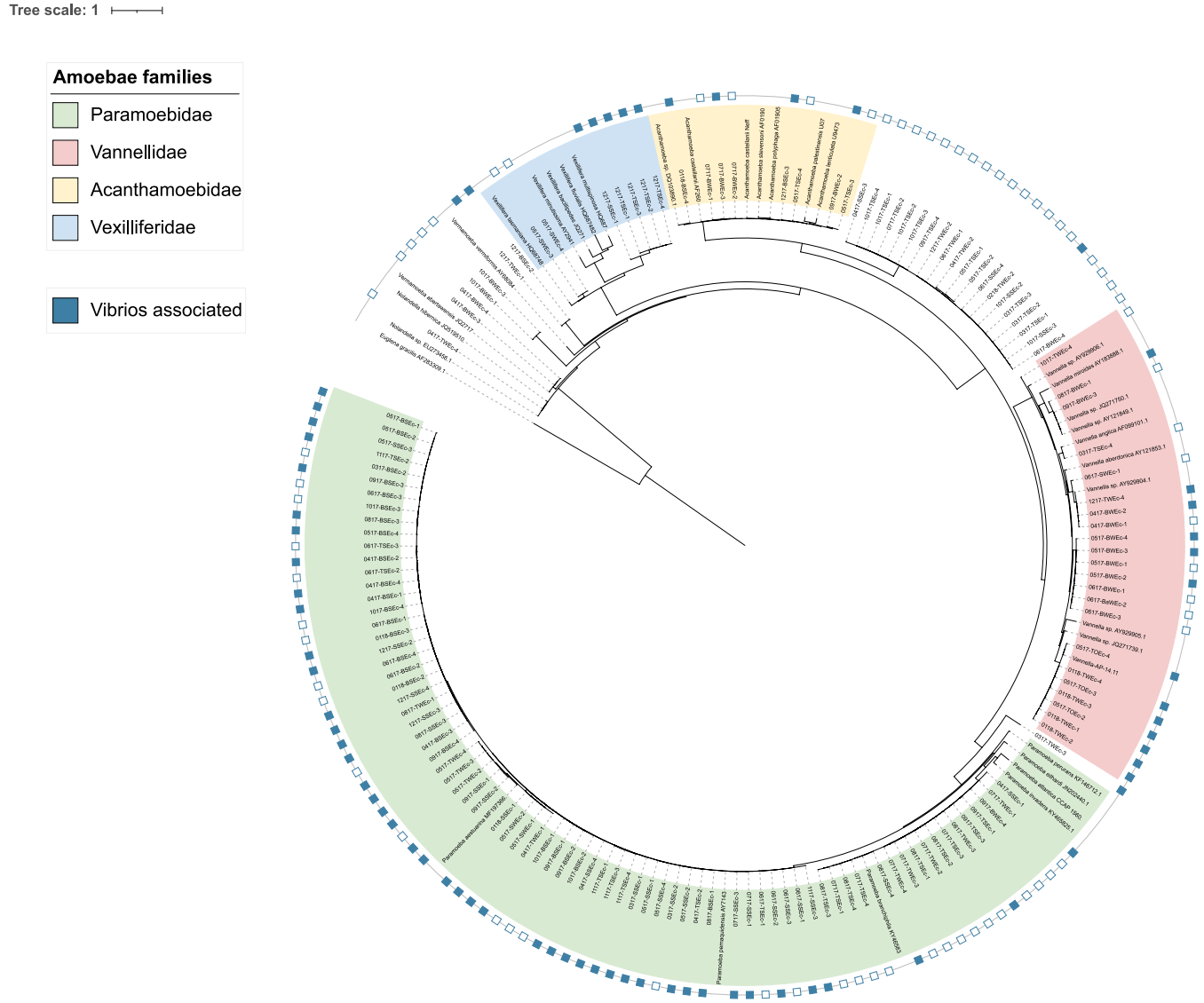

FIGURE 7 | Vibrios are frequently associated with Paramoebidae in the environment. A maximum likelihood phylogenetic tree was constructed using IQ-TREE (GTR + F + I + R3 substitution model) from an alignment of the v4 18S rDNA sequence of 175 amoebae (including 34 reference sequence and 141 amoebae from the Vibram collection) generated with ClustalW. The scale bar represents the number of nucleotide substitution per site. Detection of vibrios by Vibrionaceae-specific qPCR is indicated by a blue square next to the corresponding amoebae sample name.

of the vibrio with latex beads, both incorporated into the same vacuole during phagocytosis, indicates that the VCV is part of the digestive compartment. This reveals that unlike *V. cholerae* (Abd et al. 2004; Van der Henst et al. 2016) *V. bathopelagicus* remains confined within the amoeba's phagosomal compartment and does not escape to colonise other cellular compartments. As demonstrated by the co-exposure experiment with GFP- and mCherry-labelled *V. bathopelagicus* (Figure 4c), the VCV initially forms through the fusion of multiple phagosomes. However, during the first 30 min of interaction the VCV ceases to receive a continuous influx of newly phagocytosed bacteria, gradually becoming an isolated compartment as indicated by the pulse-chase experiment with the GFP and mCherry-labelled vibrios (Figure 4d). It remains to be determined whether the isolation of the VCV results from a progressive maturation of the phagosome over time, preventing its fusion with other phagosomal compartments (Desjardins et al. 1997) or if *V. bathopelagicus* is disturbing intracellular trafficking. This suggests that the presence of vibrios may influence the vacuole's capacity to fuse with other cellular compartments. Our observations reveal that, despite VCV acidification, some *V. bathopelagicus* remains fully viable and motile within this compartment. This is consistent with our findings that *V. bathopelagicus* can proliferate in acidic conditions in vitro, with a pH threshold for growth between 4 and 5. However, it remains unclear whether the level, timing, or frequency of this acidification is affected by the vibrio. While *V. bathopelagicus* appears to withstand acidic conditions, various studies have shown that vibrios typically evade or disrupt phagosome acidification. For instance, *V. cholerae* avoids acidification within *A. castellanii* by escaping the phagosomal compartment. However, the specific cellular compartment it colonises remains debated, with studies suggesting either the contractile vacuole (Van der Henst et al. 2016) or the amoeba's cytosol (Abd et al. 2004). Interestingly, Van der Henst et al. (2016) observed that, rather than being directed to the contractile vacuole, a subset of *V. cholerae* was able to survive within

phagosomes before being released via exocytosis. However, it remains to be determined whether this survival is linked to Vibrio-mediated interference with phagosome acidification (Van der Henst et al. 2016). In contrast, *V. parahaemolyticus* can interfere with lysosomal acidification through the T3SS effector VopQ, which binds to the V0 complex of the V-ATPase, leading to proton leakage from the lysosome (Sreelatha et al. 2013). Beyond the *Vibrio* genus, other bacteria have developed distinct strategies to handle phagosomal acidification. *Legionella pneumophila* delays phagosome-lysosome fusion during the early stage of infection (Horwitz and Maxfield 1984; Sturgill-Koszycki and Swanson 2000). Meanwhile, *Coxiella burnetii*, the causative agent of Q fever, replicates within an enlarged phagolysosome called the Coxiella-containing vacuole (CCV) which strikingly possesses lysosomal characteristics such as an acidic pH (Voth and Heinzen 2007). While some bacteria use mechanisms to escape the acidity of the phagosome, others such as *V. bathopelagicus* follow a different strategy as they are able to tolerate this hostile environment. Moreover, the increase in *V. bathopelagicus* load within the VCV over 4 h of interaction (Figure 4a) could be attributed to vibrio multiplication as evidenced by the observation of bacterial septa within the vacuole and the increase in vibrio load detected by qPCR between 2 and 8 h of interaction. These observations suggest that the VCV provides a suitable environment for bacterial growth. Several studies have documented vibrios' ability to multiply within amoebae (Abd et al. 2004; Sandström et al. 2010; Van der Henst et al. 2016). Our findings further support the potential role of amoebae as a replicative niche for vibrios. Viable *V. bathopelagicus* is then eventually released into the environment through exocytosis from a neutralised VCV, with no apparent damage to the amoeba host. In amoebae, once digestion is complete, the pH of the food vacuole increases, leading to a neutralised compartment called the post-lysosome, from which undigested residues are ultimately regurgitated via exocytosis (De Duve and Wattiaux 1966; Dunn et al. 2018). Our results strongly suggest that *V. bathopelagicus* survives and persists intracellularly despite the ongoing phagosome process, before being expelled through exocytosis, a route typically dedicated to waste products in amoebae. Various mechanisms of vibrio escape from amoebae have been described in the literature. Consistent with our findings, Van der Henst et al. reported that *A. castellanii* can release viable vibrios from the phagosome by exocytosis (Van der Henst et al. 2016). In contrast, Espinoza et al. observed that *A. castellanii* expels undigested vibrios in expelled food vacuoles (EFVs) (Espinoza-Vergara et al. 2019). These observations suggest that vibrios can adopt different strategies to exit amoebae and access the extracellular environment. Despite the apparent conservation of the various steps of phagocytosis during *P. atlantica–V. bathopelagicus* interaction, it remains unclear whether certain molecular mechanisms of this process are actively or passively affected by *V. bathopelagicus* to promote its intracellular survival. Additionally, the potential involvement of specific host factors in response to this interaction remains to be clarified.

Interestingly, the *V. bathopelagicus* Pa22 strain exhibited a significantly lower frequency of VCV formation compared to *V. bathopelagicus* Sal10, suggesting that Sal10 is more effective at colonising/maintaining itself within the amoeba and demonstrating the intra-species variability of Vibrio–amoebae interaction. This discrepancy suggests potential phenotypic adaptations, likely shaped by the prolonged interaction of Pa22 with its amoebal host. Over time, Pa22 may have modulated its intracellular behaviour, likely resulting in an attenuated phenotype. Analysis of *V. bathopelagicus* Pa22 virulome revealed some virulence genes known to be involved in vibrio's resistance to amoebae predation, such as *copA*, involved in *V. tasmaniensis* LGP32 resistance to *Vannella* sp. AP1411 (Robino et al. 2020), or the MARTX toxin involved in *V. vulnificus* resistance against *Neoparamoeba pemaquidensis* (Lee et al. 2013). Both of these genes are also present in the *V. bathopelagicus* Sal10 genome (Lasa et al. 2021 and Table S4). Comparative analysis of Pa22 and Sal10 virulomes revealed a large pool of shared potential virulence genes, except for differences in capsule/O-antigen composition and for the presence of an additional type 6 secretion system (T6SS) in the Sal10 genome. Though these differences, and certainly others, may contribute to variations in initial phagocytosis or intracellular survival between the two strains (Oyanedel et al. 2020), the isolation and characterisation of additional strains of *V. bathopelagicus* are necessary to fully elucidate the factors driving differences in VCV formation frequency. Given that only two *V. bathopelagicus* strains are currently available, *P. atlantica* was exposed to a broader panel of vibrios strains to identify common genetic determinants involved in this interaction and to assess whether this phenotype is conserved across *Vibrio* species. This panel included eight additional strains varying in phylogenetic proximity to *V. bathopelagicus*: some belonging to the Splendidus clade (the same clade as *V. bathopelagicus*), while others were from the Harveyi or Anguillarum clades. Surprisingly, the results revealed that the ability to colonise and persist within a VCV is conserved across all vibrios species tested, including those that are phylogenetically distant from *V. bathopelagicus*, suggesting that this property is widespread among vibrios. However, the observed variations in VCV formation frequency could reflect differences in host colonisation efficiency or intracellular survival among strains. Attempts at comparative genomics analysis between strains with low (4 strains) and high (6 strains) VCV formation frequency did not identify any common genetic determinants associated with increased VCV frequency, suggesting that this enhanced phenotype is likely multifactorial. Vibrios are opportunistic bacteria that can encounter and/or colonise a wide range of hosts (Takemura et al. 2014). As demonstrated by several authors (Rubio et al. 2019; Park et al. 2020; Oyanedel et al. 2023) a common phenotype in a defined host may not result from shared genetic determinants across bacterial strains, but rather from a combination of distinct virulence factors shaped by the type of host (e.g., type of protozoa or animals) encountered during their evolutionary history and by the frequency of these interactions. Thus, the enhanced ability of certain vibrios strains to colonise *P. atlantica* may have arisen from distinct evolutionary trajectories. It should be noted that, because this type of analysis focuses on the presence or absence of genetic determinants, it does not capture all the potential polymorphisms and variations in the regulation of gene expression underlying phenotypic differences between strains.

V. bathopelagicus has demonstrated a strong potential for virulence in juvenile oyster and exhibits cytotoxicity towards haemocytes, the oyster immune cells. Within the Splendidus clade, the virulence potential of vibrios strains towards oyster

is primarily attributed to their cytotoxic effects on haemocytes (Rubio et al. 2019) and relies on virulence factors also identified in the *V. bathopelagicus* genome, such as a T6SS (located to the first chromosome) (Rubio et al. 2019), the copper-efflux pump *copA* (Vanhove et al. 2016) or the exported protein of unknown function R5.7 (Bruto et al. 2018). This shows that the two strains of *V. bathopelagicus* share properties with the virulent populations of the Splendidus clade. It should be noted that no universal virulence repertoire has yet been identified for vibrios of the Splendidus clade. While the coincidental selection hypothesis suggests that amoeba predation can drive the selection of virulence traits in bacteria (Molmeret 2005), our findings do not indicate a correlation between resistance to predation by *P. atlantica* and virulence in oysters across the vibrio species tested. Bacterial host range depends on the repertoire of virulence factors generated during their evolutionary history. Indeed, these factors may not be universally effective across different host species (Robino et al. 2020) and can even have the opposite effect depending on the host (Hoque et al. 2022; Klose and Mekalanos 1998; Oyanedel et al. 2020; Zhang et al. 2014). Although avirulent vibrio strains in oysters possess the virulence factors required for survival in amoebae, they may lack the specific genetic repertoire necessary for virulence in oysters.

The ability of *V. bathopelagicus* to persist, replicate, and exit the amoebae without lysing its host—evidenced by both cellular and populational observations—supports the notion of a commensal partnership. By avoiding host lysis, the vibrio gains a significant ecological advantage, ensuring that the amoeba population remains a stable niche, which in turn facilitates the environmental dissemination of vibrios. The stability of the relationship established between *V. bathopelagicus* and *P. atlantica*, which have coexisted for years without either partner being compromised, demonstrates that an equilibrium can be established and maintained over time between an amoeba and an opportunistic bacterium such as a vibrio. Although we have shown that distinct *Vibrio* species can survive within *P. atlantica*, for this phenotype to be ecologically significant, the two partners—vibrio and amoeba—must not only be 'compatible' but also encounter each other in their natural environment. As defined by Combes (2001) in its long-term interactions paradigm, both compatibility and encounter filters play a crucial role in determining the ecological impact of such interactions (Combes 2001). Screening of the Vibram collection using a Vibrionaceae specific-qPCR (Figure 7) confirmed that vibrios and Paramoebidae do co-occur in aquatic environments. Vibrios are known to shift ecological niches depending on the season and can inhabit sediments during colder periods in Mediterranean farming ecosystems (Lopez-Joven et al. 2018) As Paramoebidae are significantly enriched in sediments (Robino et al. 2025), and thus spatially and temporally overlap with *Vibrio*, they may play a role in maintaining this seasonal reservoir, thereby promoting vibrios' persistence. Nonetheless, the survival of vibrios in other *Paramoeb*idae genera and species must be investigated to fully understand the extent of this interaction.

Overall, our results highlight a naturally occurring vibrio-amoeba interaction and suggest that *Paramoeba atlantica* can act as an environmental reservoir for vibrios, facilitating their persistence and dissemination while providing a replicative niche. As such, it may play a significant role in the ecological success of vibrios. Whether this intracellular niche substantially influences the evolutionary dynamics of vibrios remains to be determined. These findings contribute to a better understanding of the ecological strategies that vibrios employ to persist and thrive in marine environments.

Author Contributions

Laura Onillon: conceptualisation, investigation, formal analysis, visualisation, data curation, writing-original draft. **Anaïs Dufau:** investigation, formal analysis, visualisation, data curation. **Vincent Delafont:** investigation, data curation, formal analysis, writing – review and editing. **Hajar Amraoui:** investigation, data curation. **Etienne Robino:** investigation, data curation. **Angélique Perret:** investigation, data curation. **Océane Romatif:** investigation, data curation, formal analysis. **Juliette Pouzadoux:** investigation, data curation, formal analysis. **Thierry Soldati:** conceptualisation, writing – review and editing. **Marie-Agnès Travers:** conceptualisation investigation, formal analysis, supervision, writing – review and editing. **Guillaume M. Charrière:** conceptualisation, investigation, formal analysis supervision, writing – review and editing, funding acquisition.

Acknowledgements

We would like to thank Luigi Vezzuli for kindly providing us the strain *V. bathopelagicus* Sal10T. We acknowledge the imaging facility MRI, member of the France-BioImaging national infrastructure supported by the French National Research Agency (ANR-10-INBS-04, 'Investments for the future'). The authors would also like to thank the Bio-Environment platform (University of Perpignan Via Domitia) for support in library preparation and sequencing. We also thank Bruno Petton and staff of IFREMER Bouin and Argenton, who contributed to animal production and delivery. We thank Laurent Intertaglia (Banuyls) for technical assistance. We are indebted to Marc Leroy from IHPE for precious technical assistance. The present study was supported, by the Ec2co-CNRS funded VibrAm and Vintage projects, by Labex CEMEB Reservib project, and by Ifremer, University of Montpellier and University of Perpignan via Domitia. This study is set within the framework of the 'Laboratoire d'Excellence (LabEx)' TULIP(ANR-10-LABX-41). Laura Onillon was supported by an Ifremer scholarship.

Ethics Statement

The animal (oyster *Crassostrea gigas*) testing followed all regulations concerning animal experimentation. The authors declare that the use of genetic resources fulfil the French regulatory control of access and EU regulations on the Nagoya Protocol on Access and Benefit-Sharing (IRCC-FR-265540).

Conflicts of Interest

The authors declare no conflicts of interest.

Data Availability Statement

The genomic data that support the findings of this study are openly available in Dataref at https://data-dataref.ifremer.fr/bioinfo/ifremer/ihpe/WGS_Vinseq/ and https://dataview.ncbi.nlm.nih.gov/object/PRJNA1219511?reviewer=3o02qdeqre3sh6pdj3j7l7sfbl.

References

Abd, H., A. Weintraub, and G. Sandström. 2004. "Interaction Between Vibrio Cholerae and *Acanthamoeba Castellanii*." *Microbial Ecology in Health and Disease* 16: 51–57. https://doi.org/10.1080/08910600410029190.

Bankevich, A., S. Nurk, D. Antipov, et al. 2012. "SPAdes: A New Genome Assembly Algorithm and Its Applications to Single-Cell Sequencing." *Journal of Computational Biology* 19: 455–477. https://doi.org/10.1089/cmb.2012.0021.

Berk, S. G., R. S. Ting, G. W. Turner, and R. J. Ashburn. 1998. "Production of Respirable Vesicles Containing Live *Legionella Pneumophila* Cells by Two Acanthamoeba spp." *Applied and Environmental Microbiology* 64: 279–286. https://doi.org/10.1128/AEM.64.1.279-286.1998.

Bolger, A. M., M. Lohse, and B. Usadel. 2014. "Trimmomatic: A Flexible Trimmer for Illumina Sequence Data." *Bioinformatics* 30: 2114–2120. https://doi.org/10.1093/bioinformatics/btu170.

Boulais, J., M. Trost, C. R. Landry, et al. 2010. "Molecular Characterization of the Evolution of Phagosomes." *Molecular Systems Biology* 6: 423. https://doi.org/10.1038/msb.2010.80.

Bruto, M., Y. Labreuche, A. James, et al. 2018. "Ancestral Gene Acquisition as the Key to Virulence Potential in Environmental Vibrio Populations." *ISME Journal* 12: 2954–2966. https://doi.org/10.1038/s41396-018-0245-3.

Cervero-Aragó, S., S. Rodríguez-Martínez, A. Puertas-Bennasar, and R. M. Araujo. 2015. "Effect of Common Drinking Water Disinfectants, Chlorine and Heat, on Free Legionella and Amoebae-Associated Legionella." *PLoS One* 10: e0134726. https://doi.org/10.1371/journal.pone.0134726.

Combes, C. 2001. *Parasitism: The Ecology and Evolution of Intimate Interactions*. University of Chicago Press.

Cordingley, J. S., R. A. Wills, and C. L. Villemez. 1996. "Osmolarity Is an Independent Trigger of *Acanthamoeba Castellanii* Differentiation." *Journal of Cellular Biochemistry* 61: 167–171. https://doi.org/10.1002/(SICI)1097-4644(19960501)61:2%3C167::AID-JCB1%3E3.0.CO;2-S.

De Duve, C., and R. Wattiaux. 1966. "Functions of Lysosomes." *Annual Review of Physiology* 28: 435–492. https://doi.org/10.1146/annurev.ph.28.030166.002251.

De Lorgeril, J., A. Lucasson, B. Petton, et al. 2018. "Immune-Suppression by OsHV-1 Viral Infection Causes Fatal Bacteraemia in Pacific Oysters." *Nature Communications* 9: 4215. https://doi.org/10.1038/s41467-018-06659-3.

Desjardins, M., N. N. Nzala, R. Corsini, and C. Rondeau. 1997. "Maturation of Phagosomes Is Accompanied by Changes in Their Fusion Properties and Size-Selective Acquisition of Solute Materials From Endosomes." *Journal of Cell Science* 110: 2303–2314. https://doi.org/10.1242/jcs.110.18.2303.

Destoumieux-Garzón, D., L. Canesi, D. Oyanedel, et al. 2020. "Vibrio –Bivalve Interactions in Health and Disease." *Environmental Microbiology* 22: 4323–4341. https://doi.org/10.1111/1462-2920.15055.

Dunn, J. D., C. Bosmani, C. Barisch, et al. 2018. "Eat Prey, Live: Dictyostelium Discoideum as a Model for Cell-Autonomous Defenses." *Frontiers in Immunology* 8: 1906. https://doi.org/10.3389/fimmu.2017.01906.

Eren, A. M., Ö. C. Esen, C. Quince, et al. 2015. "Anvi'o: An Advanced Analysis and Visualization Platform for 'Omics Data." *PeerJ* 3: e1319. https://doi.org/10.7717/peerj.1319.

Espinoza-Vergara, G., P. Noorian, C. A. Silva-Valenzuela, et al. 2019. "*Vibrio Cholerae* Residing in Food Vacuoles Expelled by Protozoa Are More Infectious In Vivo." *Nature Microbiology* 4: 2466–2474. https://doi.org/10.1038/s41564-019-0563-x.

Fields, B. S., G. N. Sanden, J. M. Barbaree, et al. 1989. "Intracellular Multiplication of *legionella pneumophila* in Amoebae Isolated From Hospital Hot Water Tanks." *Current Microbiology* 18: 131–137. https://doi.org/10.1007/BF01570838.

García, M. T., S. Jones, C. Pelaz, R. D. Millar, and Y. Abu Kwaik. 2007. "*Acanthamoeba polyphaga* Resuscitates Viable Non-Culturable *Legionella pneumophila* After Disinfection." *Environmental Microbiology* 9: 1267–1277. https://doi.org/10.1111/j.1462-2920.2007.01245.x.

Garnier, M., Y. Labreuche, and J.-L. Nicolas. 2008. "Molecular and Phenotypic Characterization of *Vibrio aestuarianus* Subsp. Francensis Subsp. Nov., a Pathogen of the Oyster *Crassostrea gigas*." *Systematic and Applied Microbiology* 31: 358–365. https://doi.org/10.1016/j.syapm.2008.06.003.

Goris, J., K. T. Konstantinidis, J. A. Klappenbach, T. Coenye, P. Vandamme, and J. M. Tiedje. 2007. "DNA-DNA Hybridization Values and Their Relationship to Whole-Genome Sequence Similarities." *International Journal of Systematic and Evolutionary Microbiology* 57: 81–91. https://doi.org/10.1099/ijs.0.64483-0.

Goulden, E. F., M. R. Hall, D. G. Bourne, L. L. Pereg, and L. Høj. 2012. "Pathogenicity and Infection Cycle of *Vibrio owensii* in Larviculture of the Ornate Spiny Lobster (*Panulirus ornatus*)." *Applied and Environmental Microbiology* 78: 2841–2849. https://doi.org/10.1128/AEM.07274-11.

Greub, G., and D. Raoult. 2004. "Microorganisms Resistant to Free-Living Amoebae." *Clinical Microbiology Reviews* 17: 413–433. https://doi.org/10.1128/CMR.17.2.413-433.2004.

Gurevich, A., V. Saveliev, N. Vyahhi, and G. Tesler. 2013. "QUAST: Quality Assessment Tool for Genome Assemblies." *Bioinformatics* 29: 1072–1075. https://doi.org/10.1093/bioinformatics/btt086.

Hagedorn, M., and T. Soldati. 2007. "Flotillin and RacH Modulate the Intracellular Immunity of Dictyostelium to *Mycobacterium marinum* Infection." *Cellular Microbiology* 9: 2716–2733. https://doi.org/10.1111/j.1462-5822.2007.00993.x.

Harris, J. B., R. C. LaRocque, F. Qadri, E. T. Ryan, and S. B. Calderwood. 2012. "Cholera." *Lancet* 379: 2466–2476. https://doi.org/10.1016/S0140-6736(12)60436-X.

Henle, J., and F. Marchand. 1910. *Von den Miasmen und Kontagien: und von den miasmatisch-kontagiösen Krankheiten (1840)*. J.A. Barth.

Hoang, D. T., O. Chernomor, A. Von Haeseler, B. Q. Minh, and L. S. Vinh. 2018. "UFBoot2: Improving the Ultrafast Bootstrap Approximation." *Molecular Biology and Evolution* 35: 518–522. https://doi.org/10.1093/molbev/msx281.

Hoque, M. M., P. Noorian, G. Espinoza-Vergara, et al. 2022. "Adaptation to an Amoeba Host Drives Selection of Virulence-Associated Traits in *Vibrio cholerae*." *ISME Journal* 16: 856–867. https://doi.org/10.1038/s41396-021-01134-2.

Horwitz, M. A., and F. R. Maxfield. 1984. "*Legionella pneumophila* Inhibits Acidification of Its Phagosome in Human Monocytes." *Journal of Cell Biology* 99: 1936–1943. https://doi.org/10.1083/jcb.99.6.1936.

Ina-Salwany, M. Y., N. Al-saari, A. Mohamad, et al. 2019. "Vibriosis in Fish: A Review on Disease Development and Prevention." *Journal of Aquatic Animal Health* 31: 3–22. https://doi.org/10.1002/aah.10045.

Kalyaanamoorthy, S., B. Q. Minh, T. K. Wong, A. Von Haeseler, and L. S. Jermiin. 2017. "ModelFinder: Fast Model Selection for Accurate Phylogenetic Estimates." *Nature Methods* 14: 587–589. https://doi.org/10.1038/nmeth.4285.

Klose, K. E., and J. J. Mekalanos. 1998. "Distinct Roles of an Alternative Sigma Factor During Both Free-Swimming and Colonizing Phases of the *Vibrio cholerae* Pathogenic Cycle." *Molecular Microbiology* 28: 501–520. https://doi.org/10.1046/j.1365-2958.1998.00809.x.

Kudryavtsev, A., J. Pawlowski, and K. Hausmann. 2011. "Description of *Paramoeba atlantica* n. sp.(Amoebozoa, Dactylopodida)—A Marine Amoeba From the Eastern Atlantic, With Emendation of the Dactylopodid Families." *Acta Protozoologica* 50: 239–253. https://doi.org/10.4467/16890027AP.11.023.0023.

Kushmaro, A., E. Banin, Y. Loya, E. Stackebrandt, and E. Rosenberg. 2001. "Vibrio Shiloi sp. Nov., the Causative Agent of Bleaching of the Coral *Oculina patagonica*." *International Journal of Systematic and*

Evolutionary Microbiology 51: 1383–1388. https://doi.org/10.1099/00207713-51-4-1383.

Lasa, A., M. Auguste, A. Lema, et al. 2021. "A Deep-Sea Bacterium Related to Coastal Marine Pathogens." *Environmental Microbiology* 23: 5349–5363. https://doi.org/10.1111/1462-2920.15629.

Laskowski-Arce, M. A., and K. Orth. 2008. "*Acanthamoeba castellanii* Promotes the Survival of *Vibrio parahaemolyticus*." *Applied and Environmental Microbiology* 74: 7183–7188. https://doi.org/10.1128/AEM.01332-08.

Le Roux, F., K. M. Wegner, and M. F. Polz. 2016. "Oysters and Vibrios as a Model for Disease Dynamics in Wild Animals." *Trends in Microbiology* 24: 568–580. https://doi.org/10.1016/j.tim.2016.03.006.

Lee, C., D. Pajuelo, A. Llorens, et al. 2013. "MARTX of *Vibrio Vulnificus* Biotype 2 Is a Virulence and Survival Factor." *Environmental Microbiology* 15: 419–432. https://doi.org/10.1111/j.1462-2920.2012.02854.x.

Lemire, A., D. Goudenège, T. Versigny, et al. 2015. "Populations, Not Clones, Are the Unit of Vibrio Pathogenesis in Naturally Infected Oysters." *ISME Journal* 9: 1523–1531. https://doi.org/10.1038/ismej.2014.233.

Letunic, I., and P. Bork. 2024. "Interactive Tree of Life (iTOL) v6: Recent Updates to the Phylogenetic Tree Display and Annotation Tool." *Nucleic Acids Research* 52: W78–W82. https://doi.org/10.1093/nar/gkae268.

Lopez-Joven, C., J.-L. Rolland, P. Haffner, et al. 2018. "Oyster Farming, Temperature, and Plankton Influence the Dynamics of Pathogenic Vibrios in the Thau Lagoon." *Frontiers in Microbiology* 9: 2530. https://doi.org/10.3389/fmicb.2018.02530.

Lyons, M. M., Y.-T. Lau, W. E. Carden, et al. 2007. "Characteristics of Marine Aggregates in Shallow-Water Ecosystems: Implications for Disease Ecology." *EcoHealth* 4: 406–420. https://doi.org/10.1007/s10393-007-0134-0.

MacPhail, D. P. C., R. Koppenstein, S. K. Maciver, R. Paley, M. Longshaw, and F. L. Henriquez. 2021. "Vibrio Species Are Predominantly Intracellular Within Cultures of Neoparamoeba Perurans, Causative Agent of Amoebic Gill Disease (AGD)." *Aquaculture* 532: 736083. https://doi.org/10.1016/j.aquaculture.2020.736083.

Mesnil, A., M. Jacquot, C. Garcia, et al. 2023. "Emergence and Clonal Expansion of *Vibrio Aestuarianus* Lineages Pathogenic for Oysters in Europe." *Molecular Ecology* 32: 2869–2883. https://doi.org/10.1111/mec.16910.

Minh, B. Q., H. A. Schmidt, O. Chernomor, et al. 2020. "IQ-TREE 2: New Models and Efficient Methods for Phylogenetic Inference in the Genomic Era." *Molecular Biology and Evolution* 37: 1530–1534. https://doi.org/10.1093/molbev/msaa015.

Molmeret, M. 2005. "Amoebae as Training Grounds for Intracellular Bacterial Pathogens." *Applied and Environmental Microbiology* 71: 20–28. https://doi.org/10.1128/AEM.71.1.20-28.2005.

Oyanedel, D., Y. Labreuche, M. Bruto, et al. 2020. "O-Antigen Structure: A Trade-Off Between Virulence to Oysters and Resistance to Grazers." *Environmental Microbiology* 22: 4264–4278. https://doi.org/10.1111/1462-2920.14996.

Oyanedel, D., A. Lagorce, M. Bruto, et al. 2023. "Cooperation and Cheating Orchestrate Vibrio Assemblages and Polymicrobial Synergy in Oysters Infected With OsHV-1 Virus." *Proceedings of the National Academy of Sciences* 120: e2305195120. https://doi.org/10.1073/pnas.2305195120.

Page, A. J., C. A. Cummins, M. Hunt, et al. 2015. "Roary: Rapid Large-Scale Prokaryote Pan Genome Analysis." *Bioinformatics* 31: 3691–3693. https://doi.org/10.1093/bioinformatics/btv421.

Park, J. M., S. Ghosh, and T. J. O'Connor. 2020. "Combinatorial Selection in Amoebal Hosts Drives the Evolution of the Human Pathogen *Legionella Pneumophila*." *Nature Microbiology* 5: 599–609. https://doi.org/10.1038/s41564-019-0663-7.

Parks, D. H., M. Imelfort, C. T. Skennerton, P. Hugenholtz, and G. W. Tyson. 2015. "CheckM: Assessing the Quality of Microbial Genomes Recovered From Isolates, Single Cells, and Metagenomes." *Genome Research* 25: 1043–1055. https://doi.org/10.1101/gr.186072.114.

Robino, E., A. Perret, C. Noel, et al. 2025. "Diversity and Predation Capacities of Amoebozoa Against Opportunistic Vibrios in Contrasting Mediterranean Coastal Environments". https://doi.org/10.1101/2025.03.14.643055.

Robino, E., A. C. Poirier, H. Amraoui, et al. 2020. "Resistance of the Oyster Pathogen *Vibrio Tasmaniensis* LGP32 Against Grazing by Vannella sp. Marine Amoeba Involves Vsm and CopA Virulence Factors." *Environmental Microbiology* 22: 4183–4197. https://doi.org/10.1111/1462-2920.14770.

Rubio, T., D. Oyanedel, Y. Labreuche, et al. 2019. "Species-Specific Mechanisms of Cytotoxicity Toward Immune Cells Determine the Successful Outcome of Vibrio Infections." *Proceedings. National Academy of Sciences. United States of America* 116: 14238–14247. https://doi.org/10.1073/pnas.1905747116.

Sampaio, A., V. Silva, P. Poeta, and F. Aonofriesei. 2022. "Vibrio spp.: Life Strategies, Ecology, and Risks in a Changing Environment." *Diversity* 14: 97. https://doi.org/10.3390/d14020097.

Sandström, G., A. Saeed, and H. Abd. 2010. "*Acanthamoeba polyphaga* Is a Possible Host for *Vibrio cholerae* in Aquatic Environments." *Experimental Parasitology* 126: 65–68. https://doi.org/10.1016/j.exppara.2009.09.021.

Saulnier, D., S. De Decker, P. Haffner, L. Cobret, M. Robert, and C. Garcia. 2010. "A Large-Scale Epidemiological Study to Identify Bacteria Pathogenic to Pacific Oyster Crassostrea Gigas and Correlation Between Virulence and Metalloprotease-Like Activity." *Microbial Ecology* 59: 787–798. https://doi.org/10.1007/s00248-009-9620-y.

Schulz, F., I. Lagkouvardos, F. Wascher, K. Aistleitner, R. Kostanjšek, and M. Horn. 2014. "Life in an Unusual Intracellular Niche: A Bacterial Symbiont Infecting the Nucleus of Amoebae." *ISME Journal* 8: 1634–1644. https://doi.org/10.1038/ismej.2014.5.

Simão, F. A., R. M. Waterhouse, P. Ioannidis, E. V. Kriventseva, and E. M. Zdobnov. 2015. "BUSCO: Assessing Genome Assembly and Annotation Completeness With Single-Copy Orthologs." *Bioinformatics* 31: 3210–3212. https://doi.org/10.1093/bioinformatics/btv351.

Sreelatha, A., T. L. Bennett, H. Zheng, Q.-X. Jiang, K. Orth, and V. J. Starai. 2013. "Vibrio Effector Protein, VopQ, Forms a Lysosomal Gated Channel That Disrupts Host Ion Homeostasis and Autophagic Flux." *Proceedings of the National Academy of Sciences* 110: 11559–11564. https://doi.org/10.1073/pnas.1307032110.

Sturgill-Koszycki, S., and M. S. Swanson. 2000. "*Legionella pneumophila* replication vacuoles mature into acidic, endocytic organelles." *Journal of Experimental Medicine* 192: 1261–1272. https://doi.org/10.1084/jem.192.9.1261.

Takemura, A. F., D. M. Chien, and M. F. Polz. 2014. "Associations and Dynamics of Vibrionaceae in the Environment, From the Genus to the Population Level." *Frontiers in Microbiology* 5: 38. https://doi.org/10.3389/fmicb.2014.00038.

Thompson, F. L., T. Iida, and J. Swings. 2004. "Biodiversity of Vibrios." *Microbiology and Molecular Biology Reviews* 68: 403–431. https://doi.org/10.1128/MMBR.68.3.403-431.2004.

Travers, M.-A., K. B. Miller, A. Roque, and C. S. Friedman. 2015. "Bacterial Diseases in Marine Bivalves." *Journal of Invertebrate Pathology* 131: 11–31. https://doi.org/10.1016/j.jip.2015.07.010.

Van der Henst, C., T. Scrignari, C. Maclachlan, and M. Blokesch. 2016. "An Intracellular Replication Niche for *Vibrio cholerae* in the Amoeba

Acanthamoeba castellanii." *ISME Journal* 10: 897–910. https://doi.org/10.1038/ismej.2015.165.

Van der Henst, C., A. S. Vanhove, N. C. Drebes Dörr, et al. 2018. "Molecular Insights Into *Vibrio cholerae*'s Intra-Amoebal Host-Pathogen Interactions." *Nature Communications* 9: 3460. https://doi.org/10.1038/s41467-018-05976-x.

Vanhove, A. S., T. P. Rubio, A. N. Nguyen, et al. 2016. "Copper Homeostasis at the Host Vibrio Interface: Lessons From Intracellular Vibrio Transcriptomics." *Environmental Microbiology* 18: 875–888. https://doi.org/10.1111/1462-2920.13083.

Vernette, C., N. Henry, J. Lecubin, C. De Vargas, P. Hingamp, and M. Lescot. 2021. "The Ocean Barcode Atlas: A Web Service to Explore the Biodiversity and Biogeography of Marine Organisms." *Molecular Ecology Resources* 21: 1347–1358. https://doi.org/10.1111/1755-0998.13322.

Voth, D. E., and R. A. Heinzen. 2007. "Lounging in a Lysosome: The Intracellular Lifestyle of *Coxiella burnetii*." *Cellular Microbiology* 9: 829–840. https://doi.org/10.1111/j.1462-5822.2007.00901.x.

Wick, R. R., L. M. Judd, C. L. Gorrie, and K. E. Holt. 2017. "Unicycler: Resolving Bacterial Genome Assemblies From Short and Long Sequencing Reads." *PLoS Computational Biology* 13: e1005595. https://doi.org/10.1371/journal.pcbi.1005595.

Ye, J., G. Coulouris, I. Zaretskaya, I. Cutcutache, S. Rozen, and T. L. Madden. 2012. "Primer-BLAST: A Tool to Design Target-Specific Primers for Polymerase Chain Reaction." *BMC Bioinformatics* 13: 134. https://doi.org/10.1186/1471-2105-13-134.

Zhang, J., T. Ketola, A.-M. Örmälä-Odegrip, J. Mappes, and J. Laakso. 2014. "Coincidental Loss of Bacterial Virulence in Multi-Enemy Microbial Communities." *PLoS One* 9: e111871. https://doi.org/10.1371/journal.pone.0111871.

Supporting Information

Additional supporting information can be found online in the Supporting Information section.